ESI

Accessible Triplet Excited States in the Photoisomerization of Allenes with Extended Conjugation

Jonathan Álvarez-García,[a] Ramón García-Lago,[a] José Lorenzo Alonso-Gómez,[a] Carlos Silva López*[a] and María Magdalena Cid*[a]

Index

1.General Methods

All reactions were carried out under argon (C-50) or nitrogen atmosphere unless otherwise stated. Reactions that required anhydrous conditions were carried out in oven-dried glassware at 120 °C for at least 12 hours. The reaction flasks were further dried by flame heating and subsequent cooling under a stream of argon or nitrogen. The transfer of solvents or anhydrous solutions was carried out using syringes or *cannulas*, dried as described and stored in a desiccator with anhydrous Tel-Tale™ Desiccant Indicating, 10-18 Mesh. Solvents were dried according to published methods and distilled before use.[1] THF was dried by distillation over sodium/benzophenone. Amines (pyrrolidine, isopropylamine, pyridine and triethylamine) were freshly distilled from CaH_2 under argon atmosphere. All other reagents were commercial compounds of the highest purity available**.**

Silica gel 60F-254 Merk and neutral aluminum oxide 60F-254 Merk were used for thin layer chromatography and were visualized by exposure to UV light (254 nm) and revealed by treatment with a solution of phosphomolybdic acid or dinitrophenylhydrazine. Merk silica gel 60 (230-240 mesh) and 507C neutral aluminum oxide Brockmann I (100-125 mesh) Aldrich were used under pressure for flash column chromatography.

^{1}H-NMR spectra were recorded at 25 ^{o}C (unless otherwise stated) on Bruker AMX-400 at 400 MHz with residual protic solvent as internal reference [$CDCl_3$, δ_H = 7.26 ppm], [CD_2Cl_2, δ_H = 5.32 ppm], [[D_6]DMSO, δ_H = 2.50 ppm], [CD_3OD, δ_H = 3.31 ppm], [CD_3CN, δ = 2.50 ppm], [[D_8]THF, δ_H = 1.72, 3.58 ppm] and [[D_6]Acetone, δ_H = 2.05 ppm].Chemical shifts (δ) are given in parts per million (ppm) and coupling constants (*J*) are given in Hertz (Hz). The proton spectra are reported as follows: chemical shift δ (multiplicity, coupling constant *J*, number of protons). The following symbols were used for the description of coupling patterns: multiplet (m), singlet (s), doublet (d), triplet (t), broad (br). ^{13}C-NMR spectra were recorded on the same spectrometer at 100 MHz at 25 ^{o}C (unless otherwise stated) with residual protic solvent as internal reference [$CDCl_3$, δ = 77.16 ppm], [[D_6]DMSO, δ = 39.52 ppm], [CD_3OD, δ = 49.00 ppm], [CD_3CN, δ = 1.32 ppm], [[D_8]THF, δ = 25.31, 67.21 ppm]] and [[D_6]Acetone, δ = 29.84, 206.26 ppm].

IR spectra were recorded on a Bruker IFS 28 EQUINOX with Fourier transformation from a thin film deposited onto a NaCl glass plate or recorded on a Nicolet 6700 IR-Turbo infrared spectrometer. Peaks are quoted in wave numbers (cm^{-1}) and their relative intensity is reported as follows: vs = very strong, s = strong, m = medium, w = weak. ECD and UV-Vis spectra were recorded on a Jasco J-815 spectropolarimeter using a one-centimetre thick quartz cuvette at 25°C. The background was always obtained against the solvent.

Mass spectra (MS) were measured on an autospecM spectrometer, Micromass, operating at 70 eV. Fragments are indicated: *m/z* (relative intensity of base peak = 100). ESI mass spectra were recorded with an APEX3 instrument. Ions were generated using a Combi MALDI--electrospray ionization (ESI) source. High-resolution mass spectra were taken on a VG Autospec instrument. Elemental analyses were performed on an Elemental Analyzer Carlo Erba 1108.

2. Synthesis of ligands

2.1. (*P*,*P*)- 9,9'-([2,2'-bipyridine]-4,4'-diyl)bis(5,7-di-tert-butyl-2-methylnona-5,6-dien-3,8-diyn-2-ol) ((*P*)-1a)

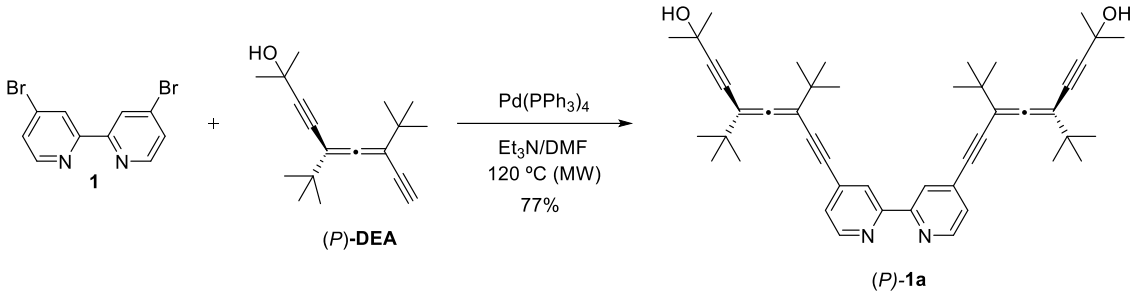

4,4'-dibromo-2,2'-bipyridine **1** (11 mg, 0.035 mmol) and $Pd(PPh_3)_4$ (5 mg, 0.004 mmol) were dissolved in dry DMF (0.65 mL) and transferred to a microwave tube previously flamed and purged with N_2. (*P*)-**DEA**[2] (20 mg, 0.077 mmol) in freshly distilled Et_3N (0.35 mL) was added. The reaction mixture was irradiated in a microwave oven (300 W, 30 psi) at 120 °C for 15 min. Then, the mixture was diluted with AcOEt and washed with distilled water (x3). The aqueous layers were extracted with DCM (x3). The combined organic layers were washed with a saturated aqueous NaCl solution and dried with Na_2SO_4 (anh). The solvent was removed under reduced pressure and the remaining solid was purified by flash chromatography (SiO_2; 80:20 Hexane/AcOEt) to give (*P*)-**1a** as a white solid (18 mg, 77%).

^{1}H NMR (400 MHz, $CDCl_3$): δ= 8.63 (d, *J* = 5 Hz, 2H; Ar-H), 8.40 (s, 2H; Ar-H), 7.34 (d, *J* = 5 Hz, 2H; Ar-H), 1.57 (s, 12H; CH_3), 1.20 (s, 18H; ^{t}Bu), 1.15 (s, 18H; ^{t}Bu).**^{13}C NMR** (100 MHz, $CDCl_3$) δ= 211.95 (C), 155.67 (C), 149.19(CH), 133.10 (C), 125.70 (CH), 123.21(CH), 103.39 (C), 102.93 (C), 97.99 (C), 90.12 (C), 88.61 (C), 75.51 (C), 65.87 (C), 35.77 (C), 35.76 (C), 31.63 (CH_3), 31.61 (CH_3), 29.17 (^{t}Bu), 29.05 (^{t}Bu). **UV/Vis** ($CHCl_3$): λ_{max} (ε)= 260.0 nm (30663 mol^{-1} dm^3 cm^{-1}), 304.0 nm (29316 mol^{-1} dm^3 cm^{-1}). **ESI-MS**: m/z calc. for $C_{46}H_{57}N_2O_2^+$ 669.4415; found 669.4415.

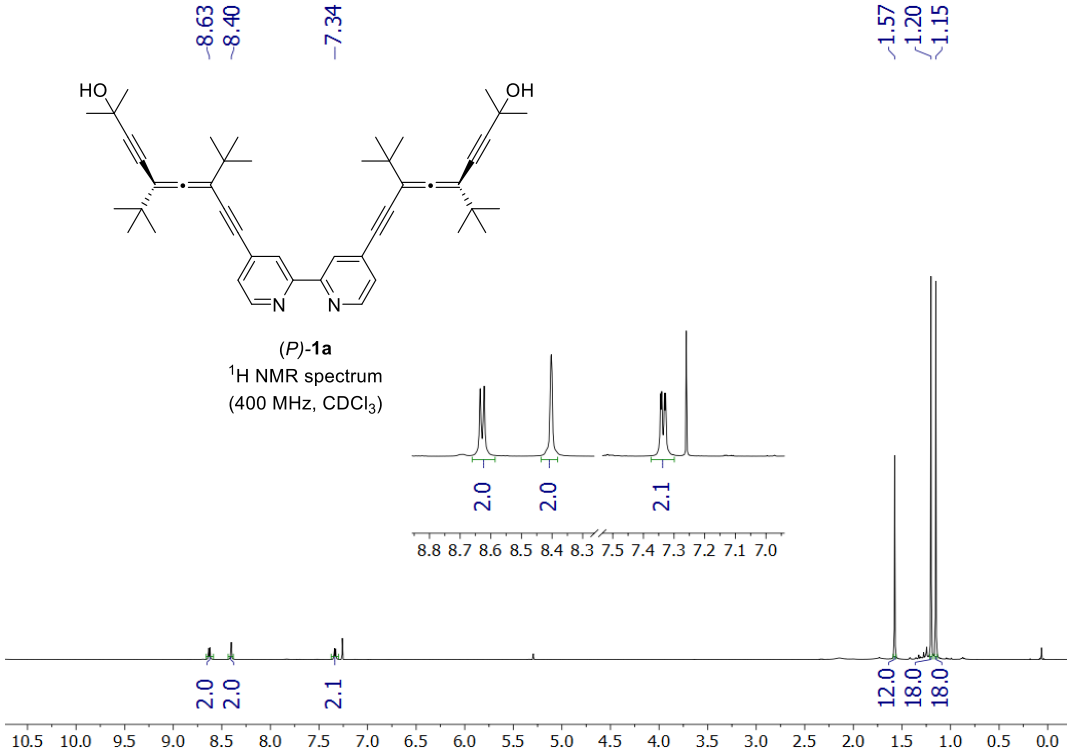

*Figure S1. (P)-**1a** ^{1}H-NMR ($CDCl_3$) spectra.*

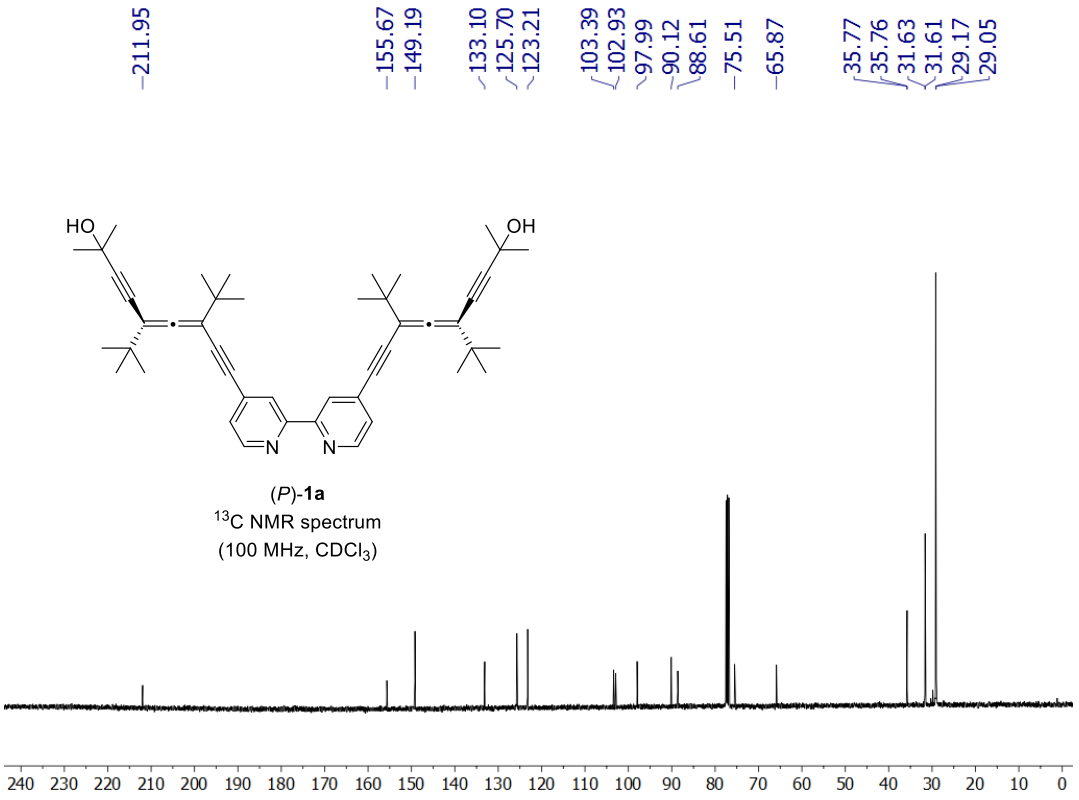

*Figure S2. (P)-**1a** ^{13}C-NMR ($CDCl_3$) spectra.*

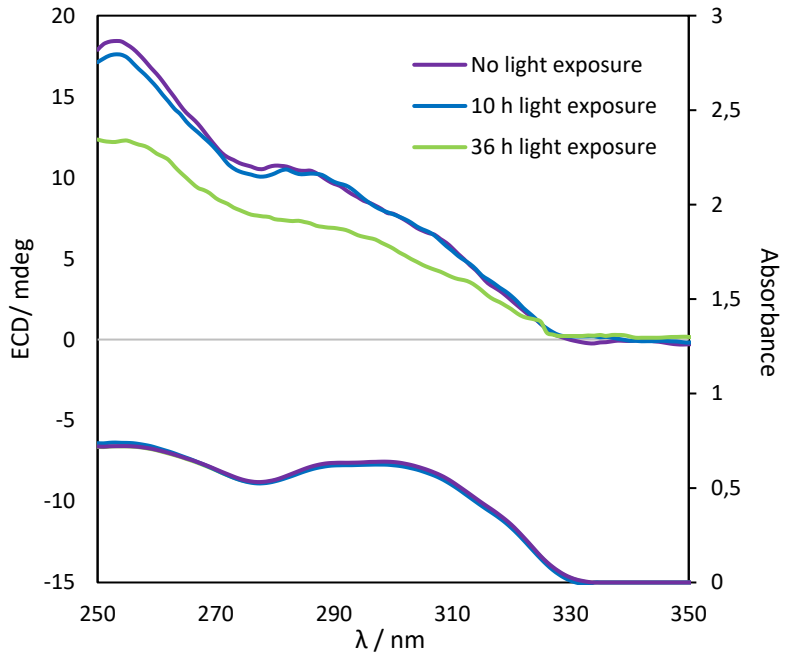

*Figure S3. Up: (P)-**1a** CD spectrum [Chloroform, 2.4·10^{-5} M]. Down: (P)-**1a** UV/Vis spectrum [Chloroform, 2.4·10^{-5} M]. Purple, blue and green lines shows changes upon light exposure and time (0 h, 10 h and 36 h respectively).*

2.2. (2Z,2'Z)-5,5'-([2,2'-bipyridine]-4,4'-diyl)bis(3-methylpent-2-en-4-yn-1-ol) ((Z)-1b)

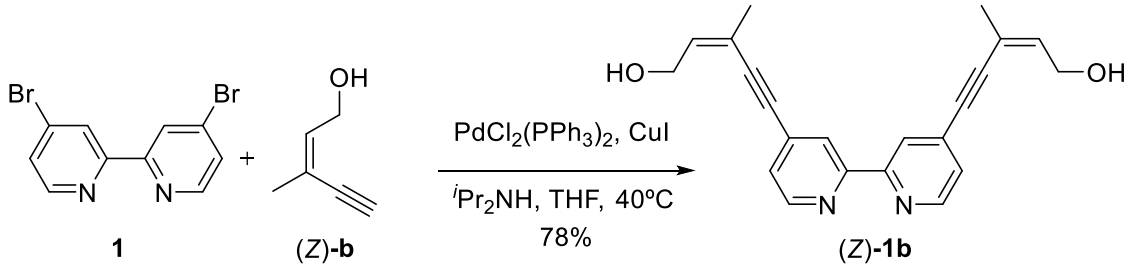

4,4'-dibromo-2,2'-bipyridine **1** (50 mg, 0.16 mmol) was dissolved in dry THF (2 mL) and transferred to a Schlenk tube previously flamed and purged with Ar. Then, (*Z*)-**b**[3] (77 mg, 0.80 mmol), $Pd(PPh_3)_2Cl_2$ (7 mg, 0.01 mmol), CuI (2 mg, 0.008 mmol) and $^{i}PrN_2H$ (56 µL, 0.40 mmol) were added. The reaction mixture was stirred at 40 °C for 4 h. The solvent was removed under reduced pressure and the remaining solid was purified by flash chromatography (SiO_2; 38:60:2 Hexane/AcOEt/Et_3N) to give **2** as a yellowish solid (43 mg, 78%).

^{1}H NMR (400 MHz, $CDCl_3$): δ= 2.00 (d, *J* = 1.1 Hz, 6H; CH_3), 4.44 (m, 4H, CH_2), 6.03 (m, 2H; C=CH), 7.32 (dd, *J* = 5.0, 1.4 Hz, 2H; Ar-H), 8.42 (s, 2H; Ar-H), 8.64 (d, *J* = 5.0 Hz, 2H; Ar-H). **^{13}C NMR** (100 MHz, $CDCl_3$): δ= 23.0 (CH_3), 61.7 (CH_2), 91.9 (C), 92.0 (C), 120.2 (C), 123.2 (CH), 125.6 (CH), 132.4 (C), 137.9 (CH), 149.3 (CH), 155.7 (C). **UV/Vis** (MeOH): λ_{max} (*ε*)= 294.0 nm (31852 $mol^{-1}\,dm^3\,cm^{-1}$), 261.0 nm (32249 $mol^{-1}\,dm^3\,cm^{-1}$). **MS** (IE): *m/z* (%): 345 (24) $[M+H]^+$, 344 (100) $[M]^+$, 343 (29) $[M-H]^+$, 316 (12), 315 (43), 301 (11). **Elemental analysis** calcd (%) for $C_{22}H_{20}N_2O_2$: C 76.72, H 5.85, N 8.13; found: C 76.27, H 5.81, N 8.14.

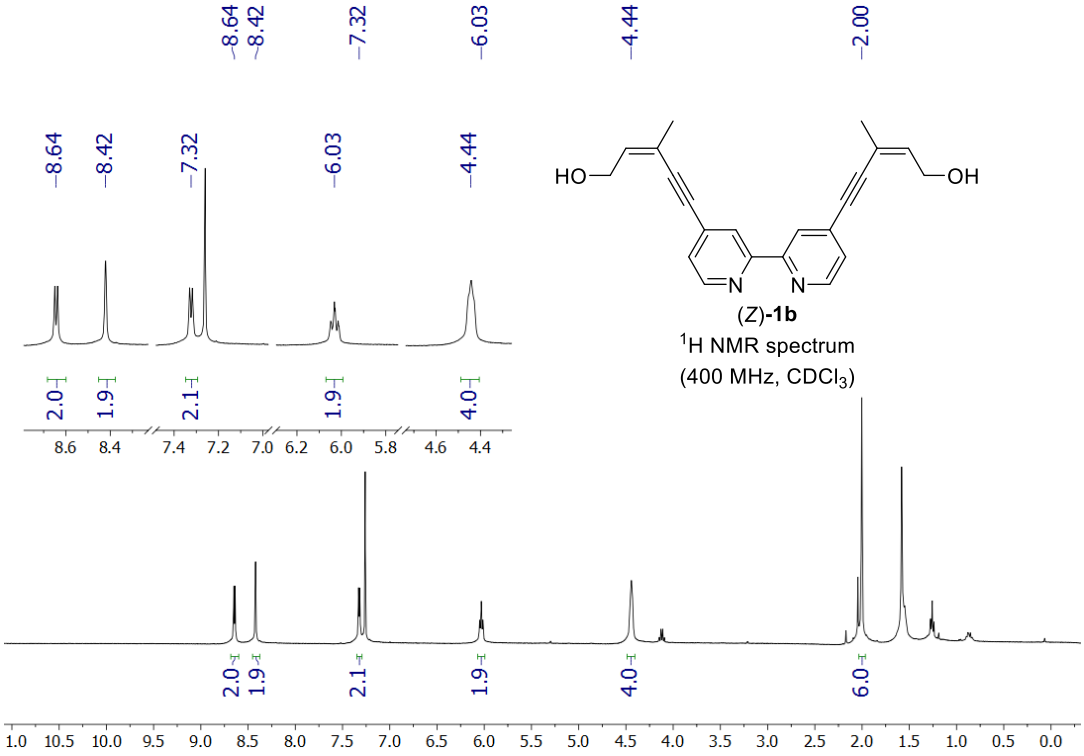

*Figure S4. (Z)-**1b** ^{1}H-NMR ($CDCl_3$) spectra.*

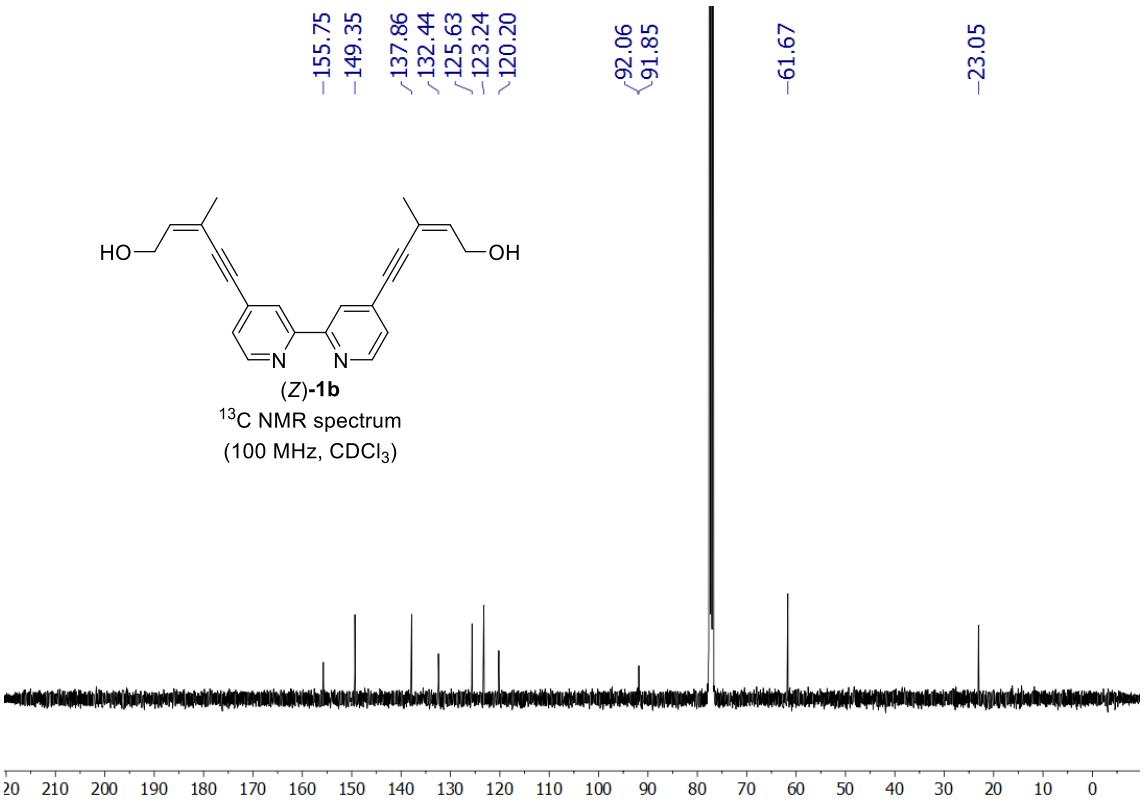

*Figure S5. (Z)-**1b** ^{13}C-NMR ($CDCl_3$) spectra.*

2.3. 4,4'-bis((E)-3-methyl-5-((trimethylsilyl)oxy)pent-3-en-1-yn-1-yl)-2,2'-bipyridine ((*E*)-1c)

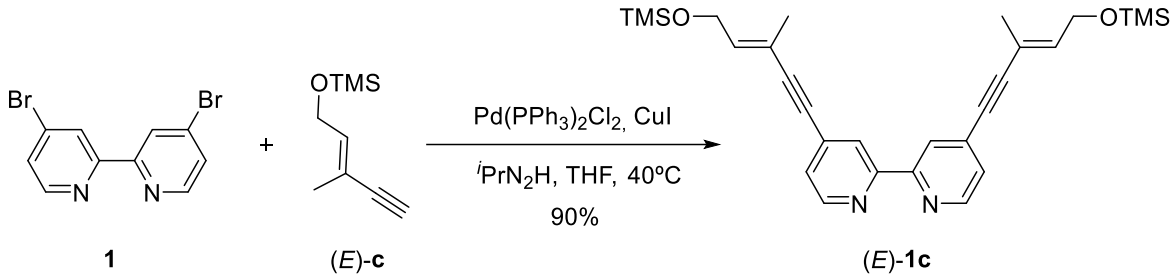

4,4'-dibromo-2,2'-bipyridine **1** (50 mg, 0.16 mmol) was dissolved in dry THF (2 mL) and transferred to a Schlenk tube previously flamed and purged with Ar. Then, silyl ether (*E*)-**c**[4] (134 mg, 0.80 mmol), $Pd(PPh_3)_2Cl_2$ (7 mg, 0.01 mmol), CuI (2 mg, 0.008 mmol) and $^{i}PrN_2H$ (54 µL, 0.40 mmol) were added. The reaction mixture was stirred at 40 °C for 1.5 h. The solvent was removed under reduced pressure and the remaining solid was purified by flash chromatography (SiO_2; 97:3 CH_2Cl_2/MeOH) to give (*E*)-**1c** as a white solid (49 mg, 90%).

^{1}H NMR (400 MHz, $CDCl_3$): δ= 0.15 (s, 18H; TMS), 1.90 (s, 6H; CH_3) 4.27 (d, *J* = 6.4 Hz, 4H; CH_2) 6.11 (t, *J* = 6.4 Hz, 2H; C=CH), 7.29 (d, *J* = 5.0 Hz, 2H; Ar-H) 8.39 (s, 2H; Ar-H), 8.61 (d, *J* = 5.0 Hz, 2H; Ar-H). **^{13}C NMR** (100 MHz, $CDCl_3$): δ= 0.41 (CH_3), 17.3 (CH_3), 59.2 (CH_2), 84.7 (C), 96.4 (C), 118.5 (C), 123.1 (CH), 125.4 (CH), 132.7 (C), 138.7 (CH), 149.1 (CH), 155.5 (C). **MS** (IE): *m/z* (%): 489 (18) $[M+H]^+$, 488 (42) $[M]^+$, 473 (21), 460 (26), 459 (66), 297 (22), 73 (100) $[TMS]^+$.

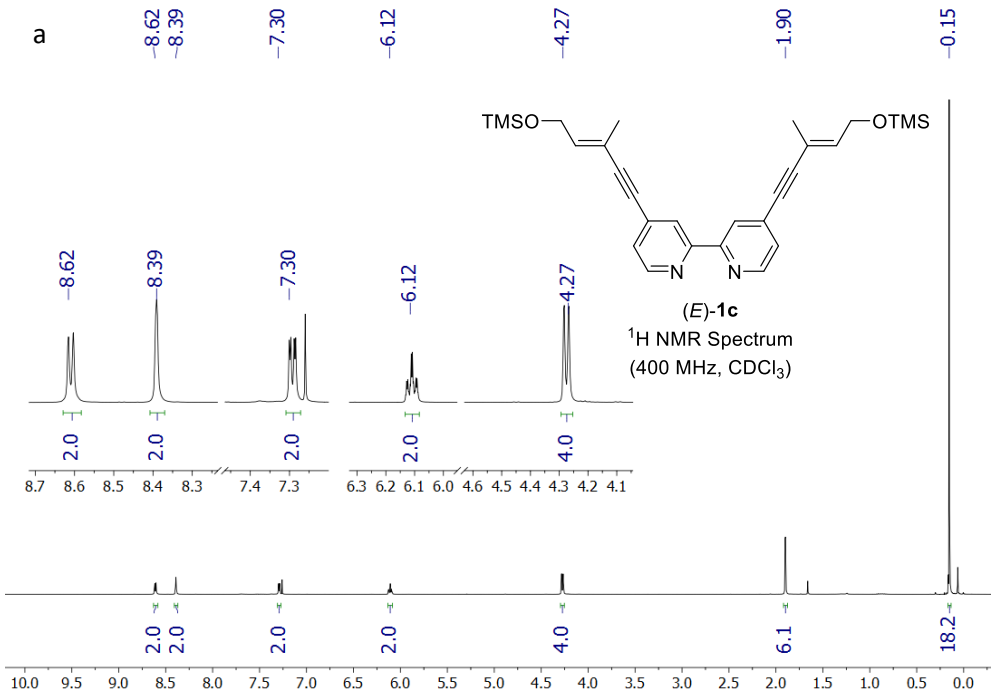

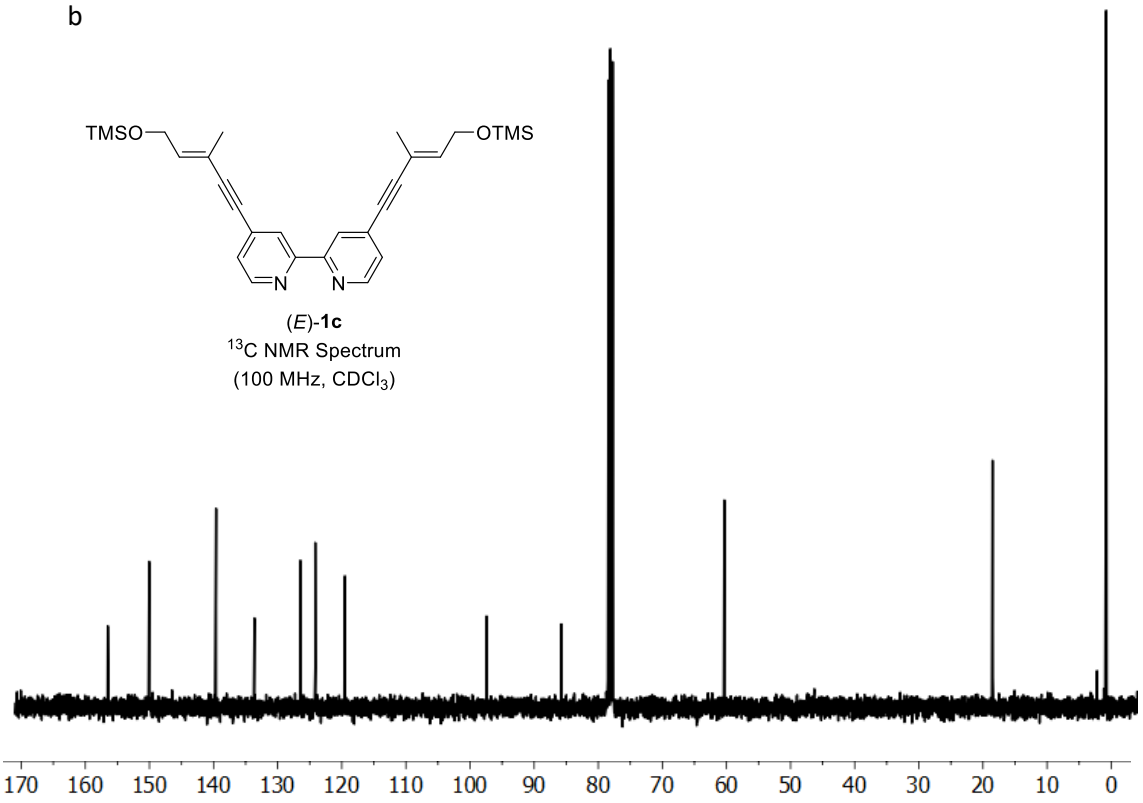

*Figure 6. a (E)-**1c** ^{1}H-NMR ($CDCl_3$) spectra, b (E)-**1c** ^{13}C-NMR ($CDCl_3$) spectra.*

2.4. (2*E*,2'*E*)-5,5'-([2,2'-bipyridine]-4,4'-diyl)bis(3-methylpent-2-en-4-yn-1-ol) ((*E*)-1b)

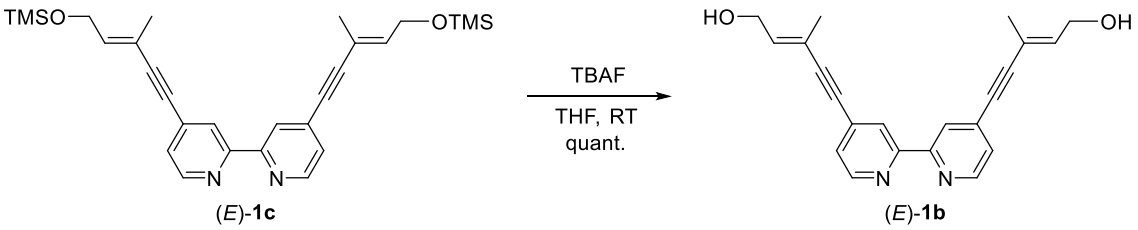

Silyl ether (*E*)-**1c** (17 mg, 0.034 mmol) was dissolved in dry THF (1.5 mL) and introduced in a round-bottom flask previously flamed and purged with Ar. TBAF (0.10 mL, 0.94 mmol) was added. The reaction mixture was stirred at room temperature for 15 min and then diluted with ^{t}BuOMe. The mixture was washed with saturated aqueous $NaHCO_3$ solution (x3). The combined aqueous layers were extracted with AcOEt (x3). The organic layers were dried with Na_2SO_4 (anh) and the solvent removed under reduced pressure. Purification by flash chromatography (SiO_2; 95:5 CH_2Cl_2:MeOH) gave (*E*)-**1b** quantitatively as a white solid. m.p: 148 °C.

^{1}H NMR (400 MHz, CD_3OD): δ= 1.93 (s, 6H; CH_3), 4.22 (d, *J* = 6.7 Hz, 4H; CH_2), 6.15 (dt, *J* = 6.7, 1.5 Hz, 2H; C=CH), 7.40 (dd, *J* = 5.0, 1.2 Hz, 2H; Ar-H), 8.29 (d, *J* = 1.2 Hz, 2H; Ar-H), 8.60 (d, *J* = 5.0 Hz, 2H; Ar-H). **^{13}C NMR** (100 MHz, CD_3OD): δ= 17.3 (CH_3), 59.2 (CH_2), 85.3 (C), 97.7 (C), 120.1 (C), 124.2 (CH), 126.8 (CH), 134.3 (C), 140.2 (CH), 150.5 (CH), 156.7 (C). **UV/Vis** (MeOH): λ_{max} (***ε***)= 294 nm (34444 $mol^{-1}\,dm^3\,cm^{-1}$), 262 nm (32407 $mol^{-1}\,dm^3\,cm^{-1}$). **MS** (IE): *m/z* (%): 345 (7) $[M+H]^+$, 344 (26) $[M]^+$, 316 (30), 315 (100), 271 (13). **Elemental analysis** calcd (%) for $C_{22}H_{20}N_2O_2$: C 76.72, H 5.85, N 8.13; found: C 76.31, H 5.77, N 8.16.

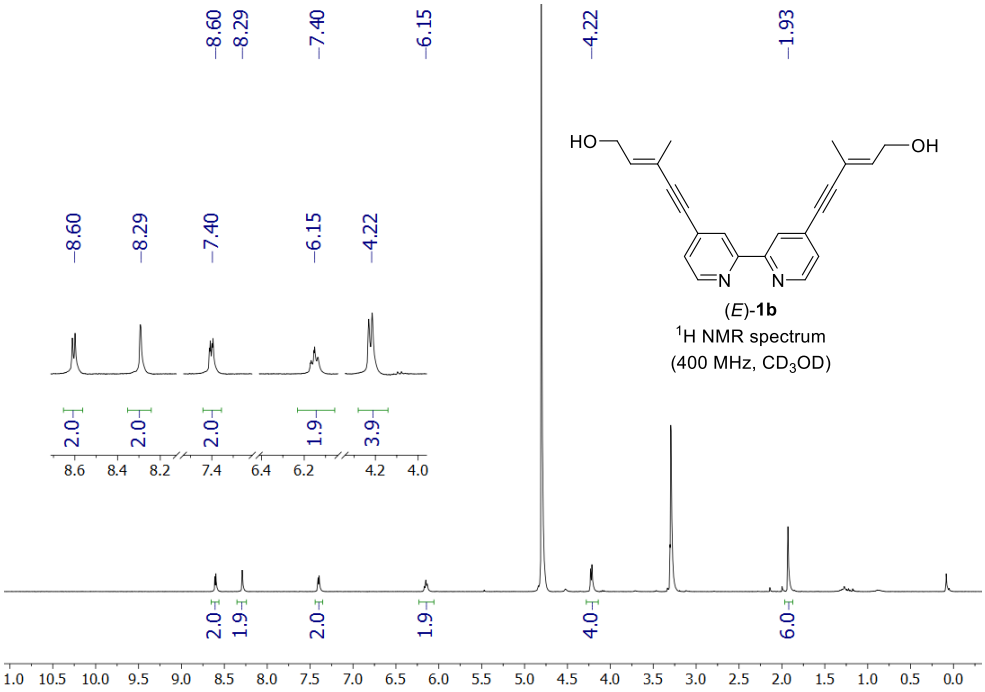

*Figure S7. (E)-**1b** ^{1}H-NMR (CD_3OD) spectra.*

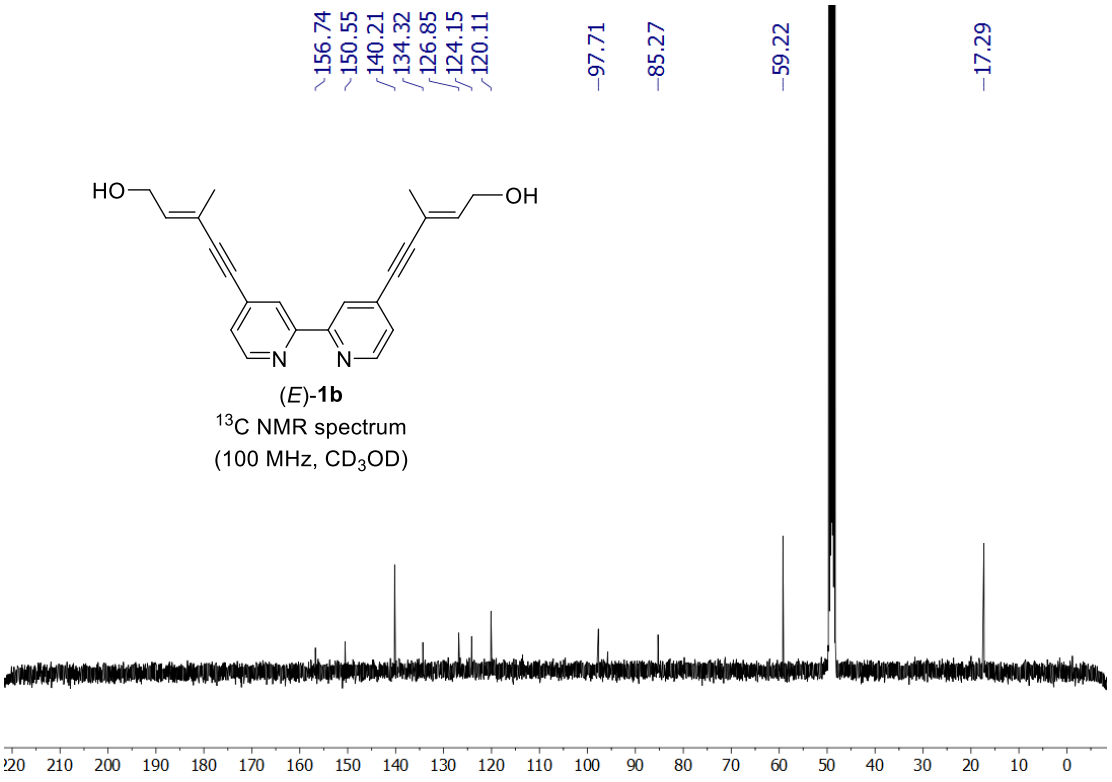

*Figure S8. (E)-**1b** ^{13}C-NMR (CD_3OD) spectra.*

2.5. (2E,2'E)-5,5'-([2,2'-bipyridine]-4,4'-diyl)bis(2-methylpent-2-en-4-yn-1-ol ((E)-1d)

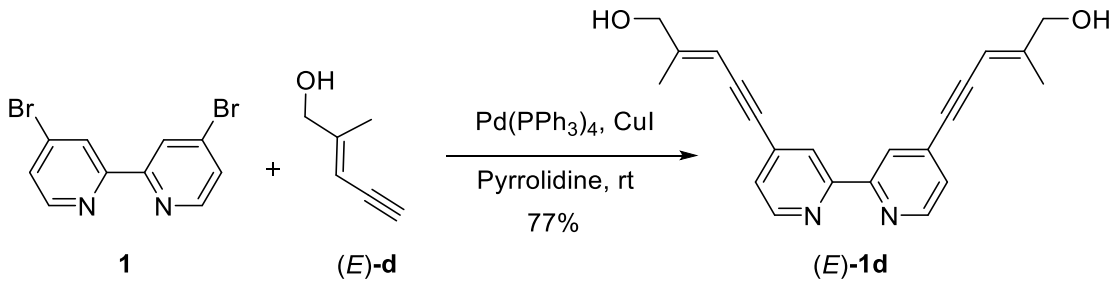

4,4'-dibromo-2,2'-bipyridine **1** (100 mg, 0.32 mmol) was dissolved in dry pyrrolidine (3 mL) and transferred to a Schlenk tube previously flamed and purged with Ar. Then, (*E*)-**d**[3] (140 mg, 1.45 mmol), $Pd(PPh_3)_4$ (19 mg, 0.016 mmol) and CuI (6 mg, 0.032 mmol) were added. The reaction mixture was stirred at room temperature for 21 h. A saturated aqueous NH_4Cl solution (3 mL) was added and the mixture was extracted with DCM (x3). The combined organic layers were dried with Na_2SO_4 (anh) and the solvent was removed under reduced pressure. Purification by flash chromatography (SiO_2; 38:60:2 Hexane/AcOEt/Et_3N) gave (*E*)-**1d** as a brown solid (79 mg, 77%).

^{1}H NMR (400 MHz, [D_6]DMSO): δ= 1.93 (s, 6H; CH_3), 4.02 (d, *J* = 5.0 Hz, 4H; CH_2), 5.18 (t, *J* = 5.0 Hz, 2H; OH), 5.84 (s, 2H; C=CH), 7.50 (d, *J* = 5.0 Hz, 2H; Ar-H), 8.32 (s, 2H; Ar-H), 8.69 (d, *J* = 5.0 Hz, 2H; Ar-H). **^{13}C NMR** (100 MHz, [D_6]DMSO): δ= 16.7 (CH_3), 64.5 (CH_2), 90.1 (C), 92.5 (C),

101.4 (CH), 121.7 (CH), 125.5 (CH), 132.2 (C), 149.8 (CH), 154.8 (C), 156.2 (C). **UV/Vis** (MeOH): λ_{max} (ε)= 299.0 nm (34871 $mol^{-1}\,dm^3\,cm^{-1}$), 266.0 nm (28510 $mol^{-1}\,dm^3\,cm^{-1}$). **MS (IE)**: *m/z* (%): 345 (15) $[M+H]^+$, 344 (55) $[M]^+$, 316 (34), 315 (100), 301 (9). **Elemental analysis** calcd (%) for $C_{22}H_{20}N_2O_2$: C 76.72, H 5.85, N 8.13; found: C 76.46, H 5.80, N 8.01.

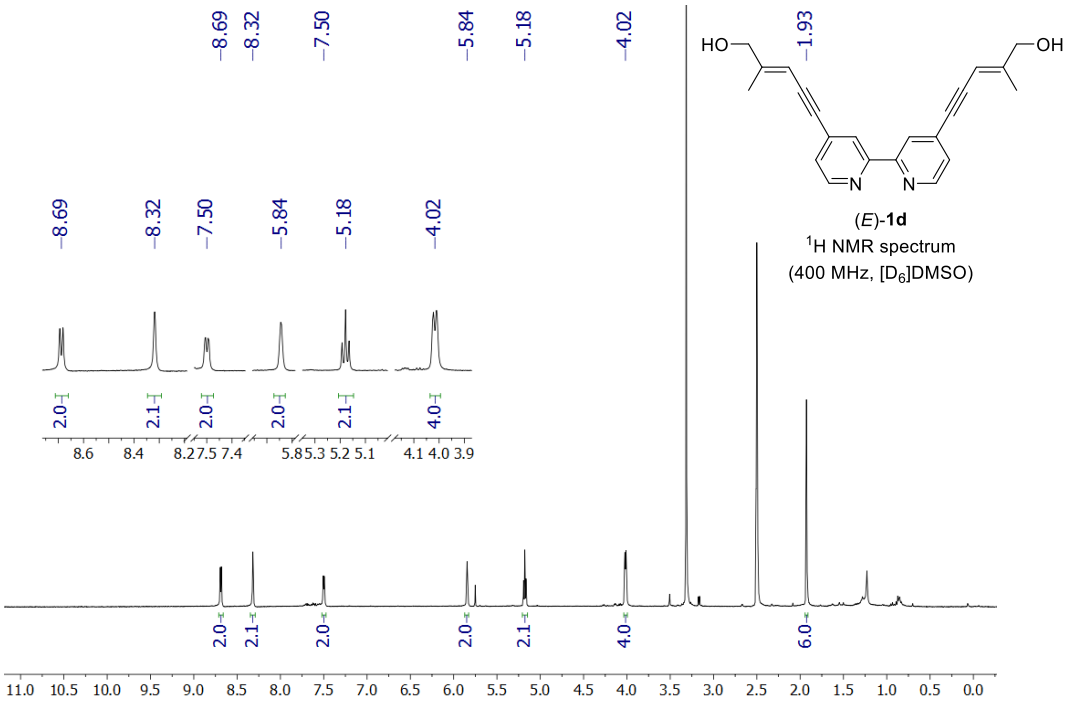

*Figure S9. (E)-**1d** ^{1}H-NMR ([D$_6$]DMSO) spectra.*

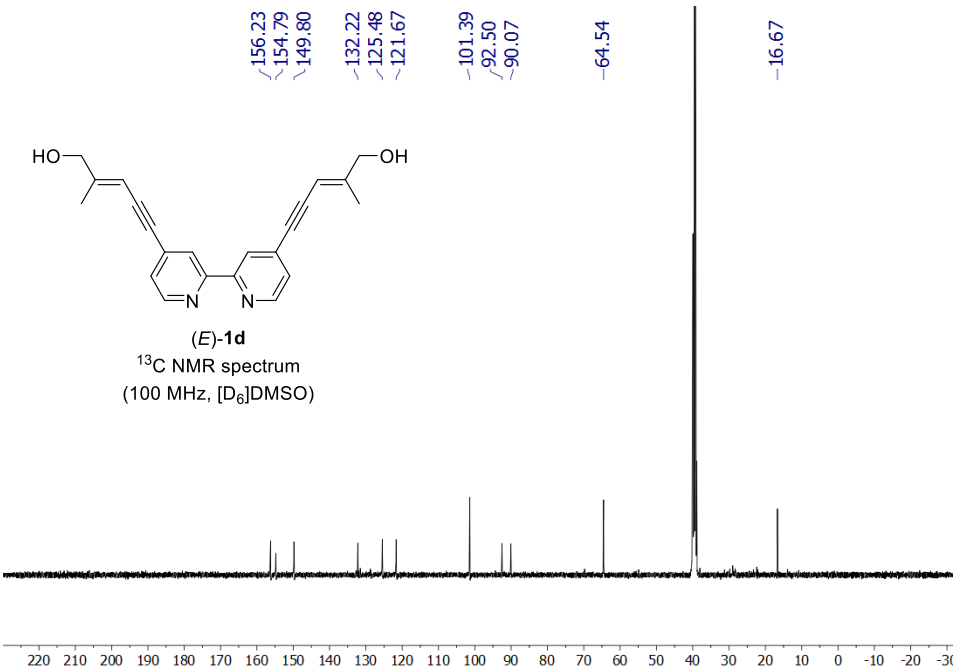

*Figure S10. (E)-**1d** ^{13}C-NMR ([D$_6$]DMSO) spectra.*

2.6. (2Z,2'Z)-5,5'-([2,2'-bipyridine]-4,4'-diyl)bis(3-methylpent-2-en-4-ynal ((*Z*)-1e)

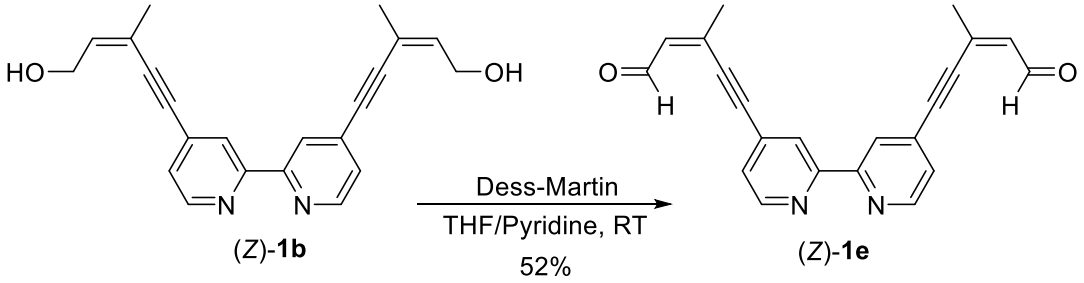

Diol (*Z*)-**1b** (176 mg, 0.51 mmol) and pyridine (0.3 mL, 3.7 mmol) were dissolved in dry THF (2 mL) and introduced in a round-bottom flask previously flamed and purged with Ar. A suspension of Dess–Martin periodinane (1.1 g, 2.54 mmol) in dry THF (6 mL) was added. The reaction mixture was stirred at room temperature for 35 h. The solvent was removed under reduced pressure and the remaining solid was redissolved in AcOEt. The mixture was washed with a saturated aqueous $NaHCO_3$ solution and then with a saturated aqueous $Na_2S_2O_3$ solution. The combined aqueous layers were extracted with AcOEt (x2) and $CHCl_3$ (x2). The combined organic layers were dried with Na_2SO_4 (anh) and the solvent removed under reduced pressure. Purification by flash chromatography (SiO_2; 98:2 CH_2Cl_2:MeOH) gave (*Z*)-**1e** as a white solid (91 mg, 52%).

^{1}H-NMR (400 MHz, $CDCl_3$): δ= 2.25 (d, *J* = 1.1 Hz, 6H; CH_3), 6.30 (m, 2H; C=CH), 7.40 (dd, *J* = 4.8, 1.4 Hz, 2H; Ar-H), 8.52 (s br, 2H, Ar-H), 8.72 (d, *J* = 5.0 Hz, 2H; Ar-H), 10.17 (d, *J* = 8.2 Hz, 2H; CHO). **^{13}C-NMR** (100 MHz, $CDCl_3$): δ= 24.7 (CH_3), 89.8 (C), 96.8 (C), 123.3 (CH), 125.8 (CH), 131.0 (C), 136.5 (CH), 140.9 (C), 149.6 (CH), 155.7 (C), 192.3 (CHO). **UV/Vis** (CH_2Cl_2): λ_{max} (ε)= 299.0 nm (57136 $mol^{-1}\,dm^3\,cm^{-1}$), 241.0 nm (36364 $mol^{-1}\,dm^3\,cm^{-1}$), 228.0 nm (36023 $M^{-1}\,cm^{-1}$). **MS** (IE): *m/z* (%): 341 (24) $[M+H]^+$, 340 (100) $[M]^+$, 339 (71) $[M-H]^+$, 311 (25), 297 (19). **Elemental analysis** calcd (%) for $C_{22}H_{16}O_2N_2$: C 77.63, H 4.74, N 8.23; found: C 77.38, H 4.71, N 8.15.

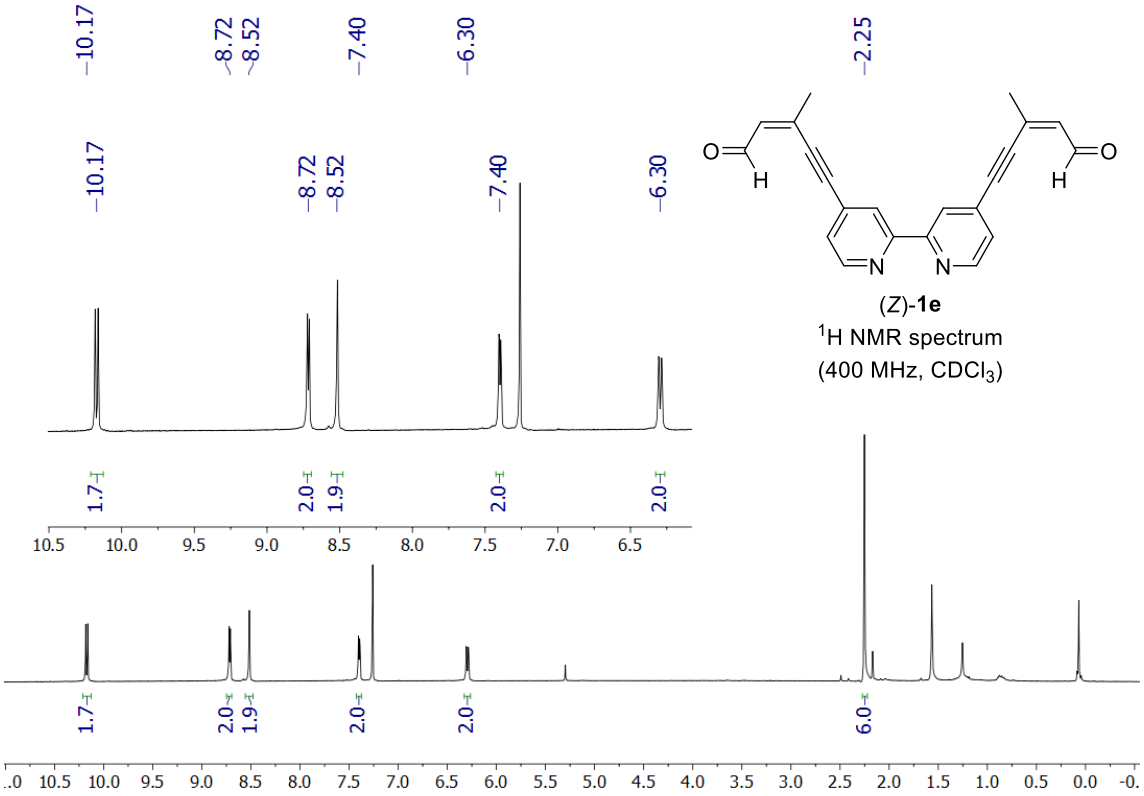

*Figure S11. (Z)-**1e** ^{1}H-NMR ($CDCl_3$) spectra.*

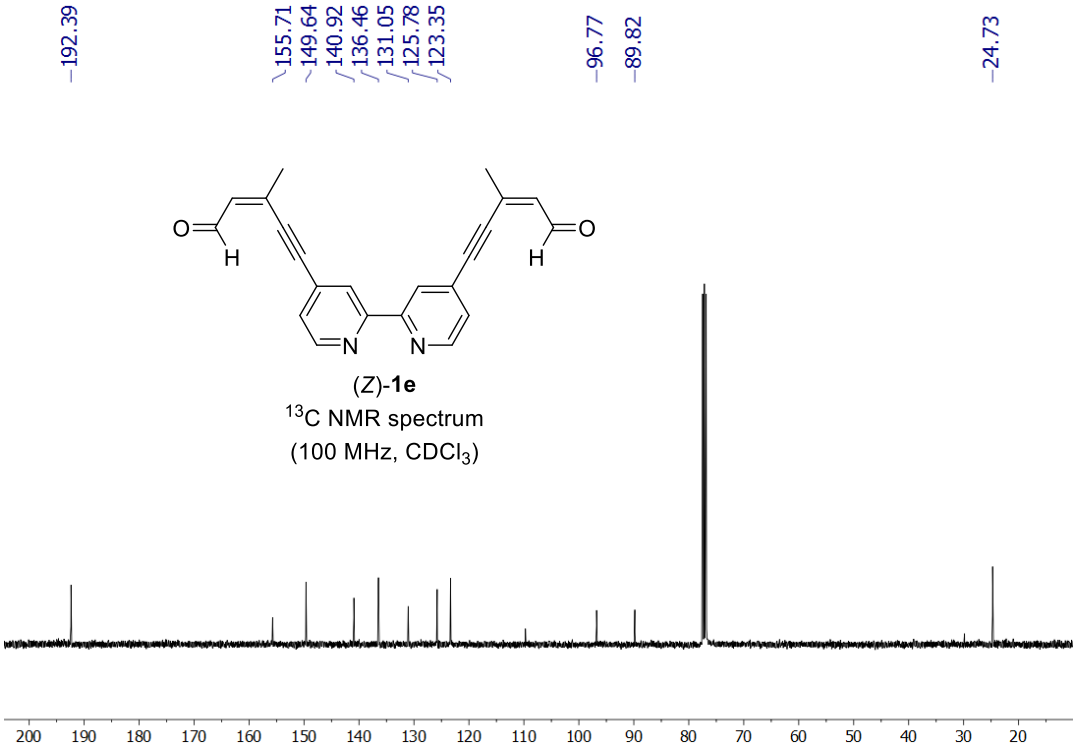

*Figure S12. (Z)-**1e** ^{13}C-NMR ($CDCl_3$) spectra.*

2.7. (Z)-3-methyl-5-(pyridin-4-yl)pent-2-en-4-yn-1-ol ((Z)-2b)

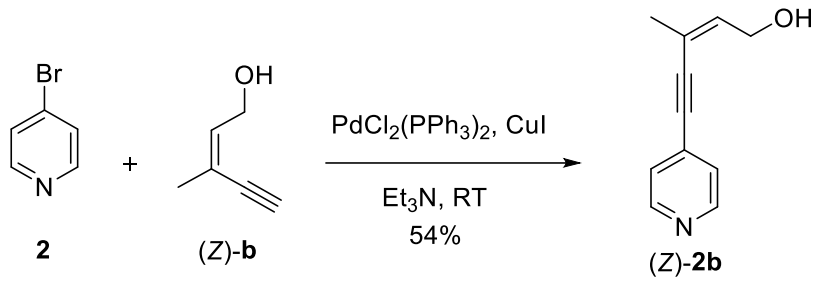

4-bromopyridine **2** (245 mg, 1.55 mmol) was dissolved in freshly distilled Et_3N (5.8 mL) and transferred to a Schlenk tube previously flamed and purged with Ar. Then, (*Z*)-**b** (224 mg, 2.33 mmol), $Pd(PPh_3)_2Cl_2$ (44 mg, 0.06 mmol) and CuI (12 mg, 0.06 mmol) were added. The reaction mixture was degassed by 3 freeze-pump-thaw cycles and finally filled with Ar. Then, the mixture was stirred at room temperature for 20 h. The solvent was removed under reduced pressure and the remaining solid was purified by flash chromatography (SiO_2; 25:75 Hexane/AcOEt) to give (*Z*)-**2b** as yellowish oil (145 mg, 54%).

^{1}H NMR (400 MHz, $CDCl_3$): δ= 1.89 (d, *J* = 1.2 Hz, 3H; CH_3), 4.33 (d, *J* = 6.8 Hz, 2H; CH_2), 5.98 (dt, *J* = 6.8, 1.2 Hz, 1H; C=CH), 7.18 (d, *J* = 5.9 Hz, 2H; Ar-H), 8.45 (d, *J* = 5.9 Hz, 2H; Ar-H). **^{13}C NMR** (100 MHz, $CDCl_3$): δ= 22.7 (CH_3), 60.9 (CH_2), 90.9 (C), 92.5 (C), 118.8 (C), 125.5 (CH), 131.7 (C), 138.9 (CH), 149.3 (CH). **UV/ Vis** (MeOH): λ_{max} (ε)= 292.0 nm (sh, 14996 $mol^{-1}\,dm^3\,cm^{-1}$); 278.0 nm (17987 $mol^{-1}\,dm^3\,cm^{-1}$). **MS** (IE): *m/z* (%): 173 (8) $[M]^+$, 172 (10) $[M\text{-H}]^+$, 155 (100), 154 (79).

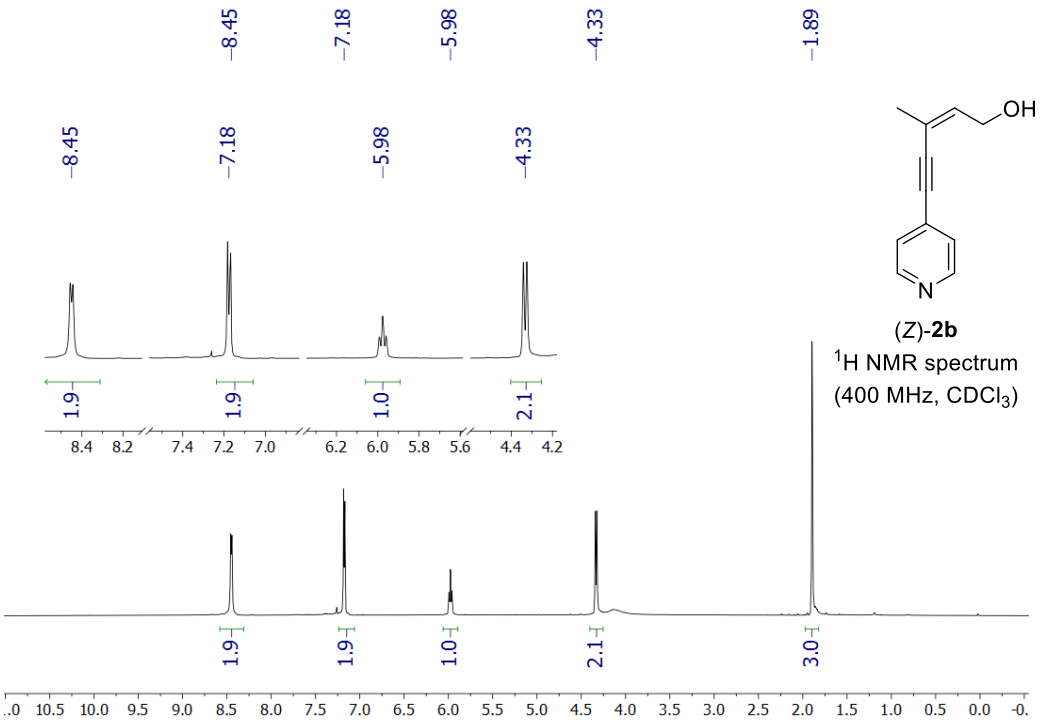

*Figure S13. (Z)-**2b** ^{1}H-NMR ($CDCl_3$) spectra.*

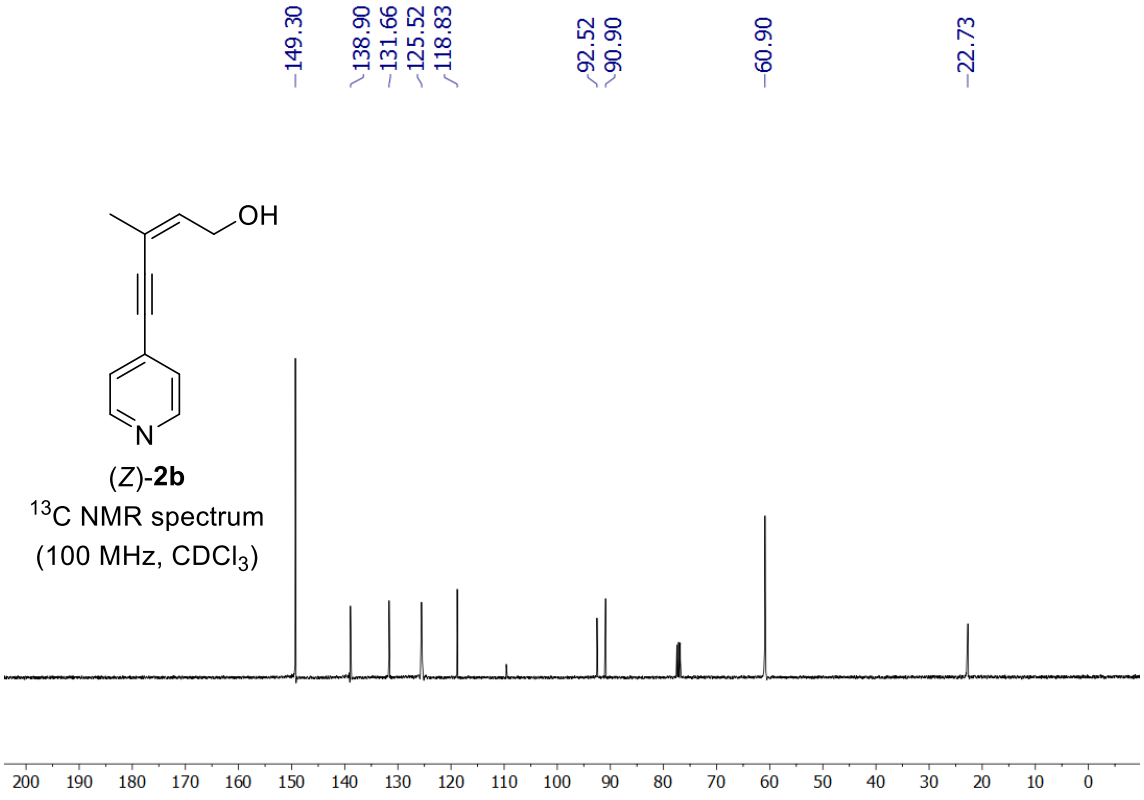

*Figure S14. (Z)-**2b** ^{13}C-NMR ($CDCl_3$) spectra.*

3. Synthesis of Re(I) complexes

3.1. Complex Re(I)-1a

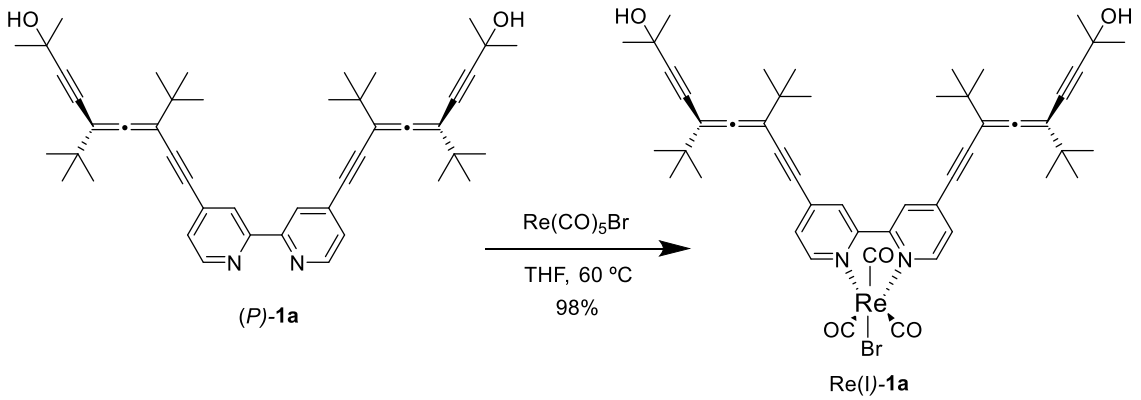

Bipyridine (*P*)-**1a** (5 mg, 0.008 mmol) and $Re(CO)_5Br$ (3 mg, 0.008 mmol) were placed in a Schlenk tube previously flamed and purged with Ar. Dry THF (3 mL) was added and the reaction mixture was stirred at 60 °C for 16 h keeping the reaction in the dark. The solvent was removed under reduced pressure to give Re(I)-**1a** (8 mg, 98%) as an orange solid.

^{1}H NMR (400 MHz, CD_3CN): δ= 8.94 (d, *J* = 5 Hz, 2H; Ar-H), 8.46 (s, 2H; Ar-H), 7.56 (d, *J* = 5 Hz, 2H; Ar-H), 1.47 (s, 12H; CH_3), 1.24 (s, 18H; ^{t}Bu), 1.18 (s, 18H; ^{t}Bu). **^{13}C NMR** (100 MHz, CD_3CN)

δ= 213.10 (C), 207.95 (CO), 198.20 (CO), 156.42 (C), 153.9 (CH), 135.53 (C), 129.65 (CH), 126.79(CH), 105.23 (C), 103.53(C), 101.06 (C), 93.51 (C), 89.50 (C), 74.34 (C), 65.59 (C), 36.51 (C), 36.46 (C), 36.44 (C), 31.73 (CH_3), 31.71 (CH_3), 29.18 (^{t}Bu), 29.02 (^{t}Bu). **UV/ Vis** ($CHCl_3$): λ_{max} (ε)= 270.0 nm (43151 mol^{-1} dm^3 cm^{-1}); 304 nm (29709 mol^{-1} dm^3 cm^{-1}); 400 nm (6380 mol^{-1} dm^3 cm^{-1}). **ESI-MS**: m/z calc. for $C_{49}H_{56}N_2O_5Re$ 939.3747; found 939.3743.

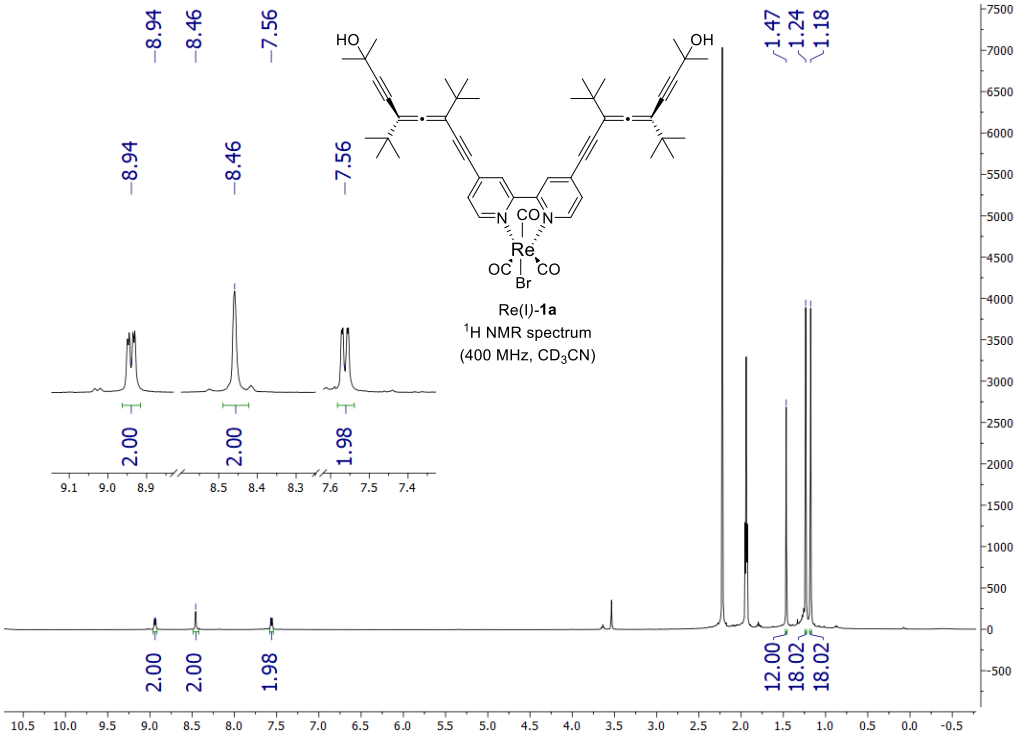

*Figure S15. Re(I)-**1a** ^{1}H-NMR (CD_3CN) spectra.*

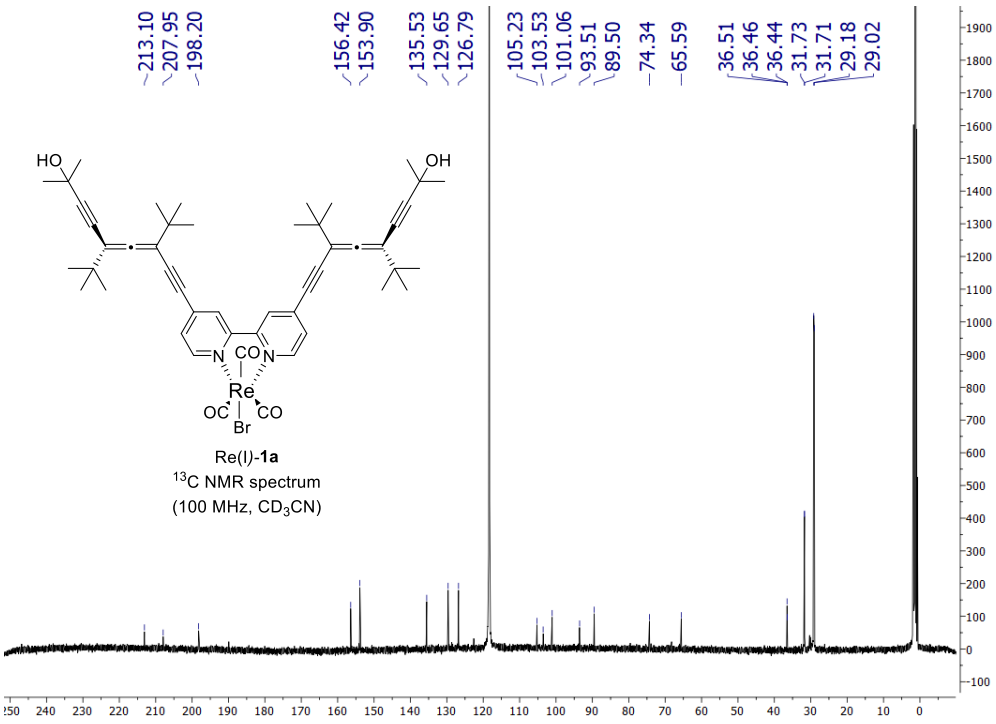

*Figure S16. Re(I)-**1a** ^{13}C-NMR (CD_3CN) spectra*

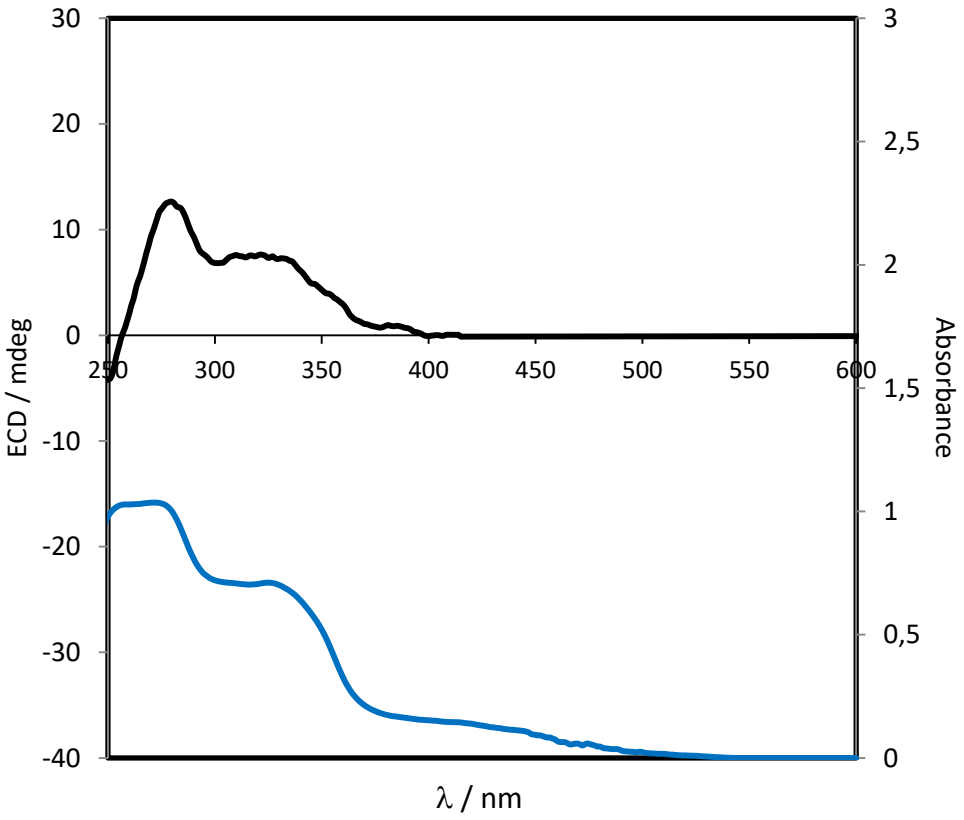

*Figure S17. Blue solid line: Re(I)-**1a** UV/Vis spectrum [Chloroform, 2.4·10^{-5} M]. Black solid line: Re(I)-**1a** CD spectrum [Chloroform, 2.4·10^{-5} M].*

Crystallographic data of Re(I)-1a

Crystals suitable for x-ray diffraction could be grown from the slow evaporation of a solution of compound Re(I)-**1a** in CD_3CN.

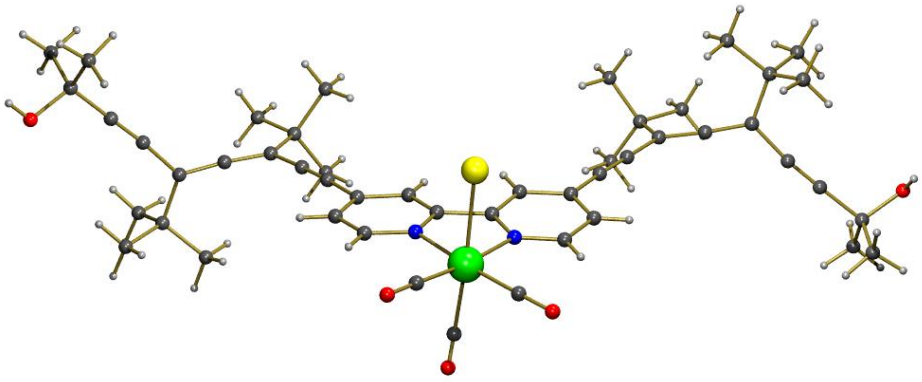

Table S1. Crystal data and structure refinement for Re(I)-**1a**

Empirical formula	$C_{51}H_{59}BrN_3O_5Re$
Formula weight	1060.12
Temperature	100.0 K

Wavelength	0.71073 Å	
Crystal system	Orthorhombic	
Space group	$I2_12_12_1$	
Unit cell dimensions	a = 15.6986(9) Å	a= 90°.
	b = 24.7762(14) Å	b= 90°.
	c = 26.3491(16) Å	g = 90°.
Volume	10248.5(10) $Å^3$	
Z	8	
Density (calculated)	1.374 Mg/m^3	
Absorption coefficient	3.196 mm^{-1}	
F(000)	4288	
Crystal size	0.214 x 0.083 x 0.077 mm^3	
Theta range for data collection	2.595 to 28.338°.	
Index ranges	-20<=h<=20, -33<=k<=32, -35<=l<=34	
Reflections collected	53772	
Independent reflections	12762 [R(int) = 0.0434]	
Completeness to theta = 25.242°	99.8 %	
Absorption correction	Semi-empirical from equivalents	
Max. and min. transmission	0.7457 and 0.5099	
Refinement method	Full-matrix least-squares on F^2	
Data / restraints / parameters	12762 / 1 / 566	
Goodness-of-fit on F^2	1.083	
Final R indices [I>2sigma(I)]	R1 = 0.0675, wR2 = 0.1456	
R indices (all data)	R1 = 0.0897, wR2 = 0.1588	
Absolute structure parameter	0.026(19)	
Extinction coefficient	n/a	
Largest diff. peak and hole	2.868 and -2.654 $e.Å^{-3}$	

3.2. Complexes Re(I)-(*Z*)-1b and Re(I)-(*E*)-1b

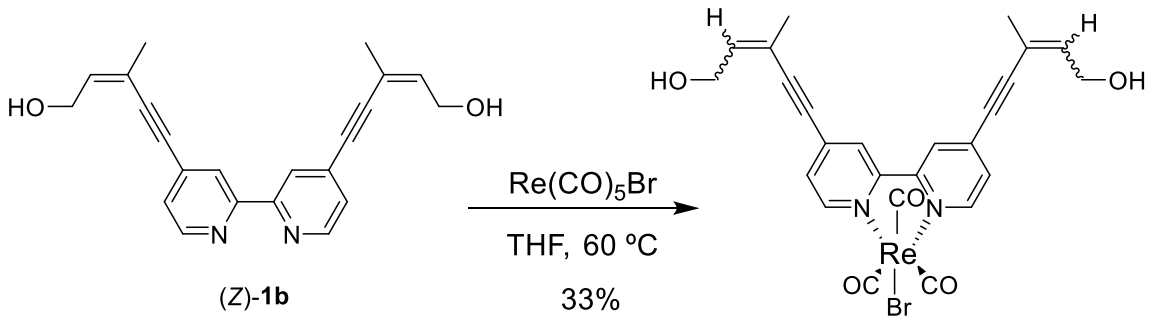

Re(I)-(*Z*)-**1b** + Re(I)-(*E*)-**1b**

Bipyridine (*Z*)-**1b** (25 mg, 0.073 mmol) and $Re(CO)_5Br$ (32 mg, 0.08 mmol) were placed in an amber round-bottom flask previously flamed and purged with Ar. Dry THF (2 mL) was added and the reaction mixture was stirred at 60°C for 5 h, keeping the reaction vessel in the dark. The solvent was removed under reduced pressure and the remaining solid was purified by flash chromatography (SiO_2; 80:20 CH_2Cl_2/ CH_3CN) to give a mixture of complexes Re(I)-(*Z*)-**1b** and Re(I)-(*E*)-**1b** as an orange solid (17 mg, 33%) in a ratio 7:1 respectively.

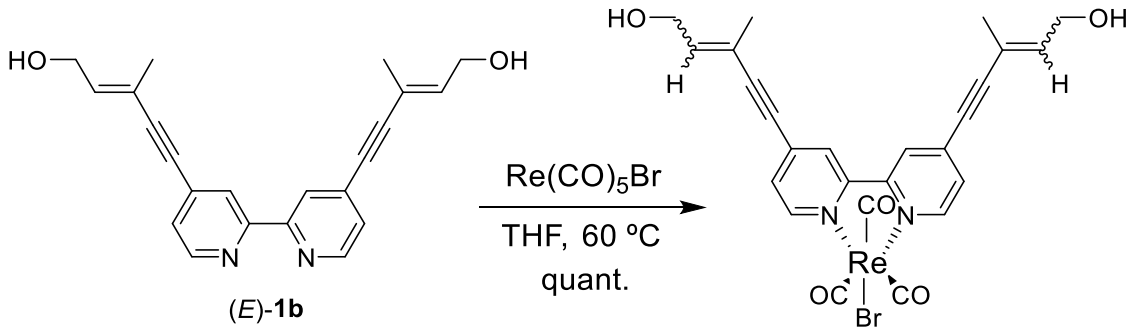

Re(I)-(*Z*)-**1b** + Re(I)-(*E*)-**1b**

Bipyridine (*E*)-**1b** (23 mg, 0.067 mmol) and $Re(CO)_5Br$ (30 mg, 0.073 mmol) were placed in an amber round-bottom flask previously flamed and purged with Ar. Dry THF (2 mL) was added and the reaction mixture was stirred at 60 °C for 5 h, keeping the reaction vessel in the dark. The solvent was removed under reduced pressure, rendering quantitatively a mixture of complexes Re(I)-(*Z*)-**1b** and Re(I)-(*E*)-**1b** as an orange solid in a ratio 1:6 respectively.

Re(I)-(*Z*)-**1b**: **^{1}H NMR** (400 MHz, $[D_6]$DMSO): δ= 1.99 (d, *J* = 1.1 Hz, 6H; CH_3), 4.27 (m, 4H; CH_2), 4.94 (t, *J* = 5.6 Hz, 2H; OH), 6.16 (m, 2H; C=CH), 7.73 (dd, *J* = 5.7, 1.4 Hz, 2H; Ar-H), 8.95 (d, *J* = 1.4 Hz, 2H; Ar-H), 8.98 (d, *J* = 5.7 Hz, 2H; Ar-H). **^{13}C NMR** (100 MHz, $[D_6]$DMSO): δ= 22.0 (CH_3), 59.8 (CH_2), 89.7 (C), 96.8 (C), 116.0 (C), 126.3 (CH), 128.9 (CH), 134.0 (C), 142.9 (CH), 153.0 (CH), 155.3 (C), 189.1 (C), 197.2 (C). **UV/ Vis** (MeOH) for *E*/*Z* isomers mixture: λ_{max} (ε)= 397.0

nm (9526 $mol^{-1}\,dm^3\,cm^{-1}$), 316.0 nm (53783 $mol^{-1}\,dm^3\,cm^{-1}$), 267.0 nm (50027 $mol^{-1}\,dm^3\,cm^{-1}$), 201.0 nm (55743 $mol^{-1}\,dm^3\,cm^{-1}$). **MS** (IE): *m/z* (%): 697 (19) $[M+H]^+$ ^{81}[Br], 696 (70) $[M]^+$ ^{81}[Br], 695 (29) $[M+H]^+$ ^{79}[Br], 694 (100) $[M]^+$ ^{79}[Br], 640 (49), 638 (80), 610 (37), 334 (14). **Elemental analysis calcd (%)** for $C_{25}H_{20}BrN_2O_5Re$: C 43.23, H 2.90, N 4.03; found: C 42.72, H 2.83, N 4.00.

Re(I)-(*E*)-**1b:** **^{1}H NMR** (400 MHz, [D_6]Acetone): δ= 1.95 (d, *J* = 1.1 Hz, 6H; CH_3), 3.98 (t, *J* = 5.5 Hz, 2H; OH), 4.29 (t, *J* = 5.5 Hz, 4H; CH_2), 6.29 (dt, *J* = 5.5, 1.1 Hz, 2H; C=CH), 7.72 (dd, *J* = 5.6, 1.2 Hz, 2H; Ar-H), 8.74 (d, *J* = 1.2 Hz, 2H; Ar-H), 9.05 (d, *J* = 5.6 Hz, 2H; Ar-H). **^{13}C NMR** (100 MHz, [D_6]Acetone): δ= 17.1 (CH_3), 59.2 (CH_2), 83.9 (C), 102.1 (C), 118.1 (C), 126.8 (CH), 129.5 (CH), 135.9 (C), 143.6 (CH), 153.9 (CH), 156.6 (C), 198.3 (CO), 224.9 (CO). **UV/ Vis** (MeOH) for *E*/*Z* isomers mixture: λ_{max} (*ε*)= 397.0 nm (9526 $mol^{-1}\,dm^3\,cm^{-1}$), 316.0 nm (53783 $mol^{-1}\,dm^3\,cm^{-1}$), 267.0 nm (50027 $mol^{-1}\,dm^3\,cm^{-1}$), 201.0 nm (55743 $mol^{-1}\,dm^3\,cm^{-1}$). **MS** (IE): *m/z* (%): 696 (19) $[M]^+$ ^{81}[Br], 695 (7) $[M+H]^+$ ^{79}[Br], 694 (24) $[M]^+$ ^{79}[Br], 640 (19), 638 (26), 346 (22), 345 (100), 344 (27). **Elemental analysis** calcd (%) for $C_{25}H_{20}BrN_2O_5Re$: C 43.23, H 2.90, N 4.03. found: C 42.72, H 2.83, N 4.00.

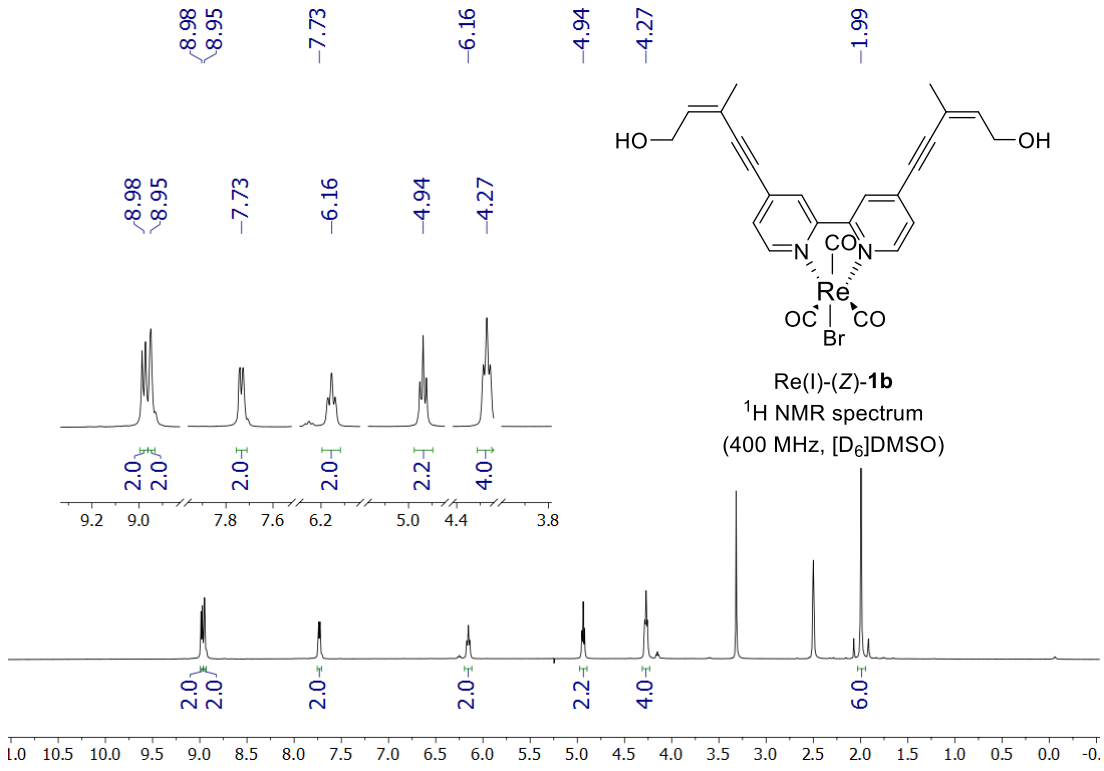

*Figure S18. Re(I)-(Z)-**1b** ^{1}H-NMR ([D_6]DMSO) spectra.*

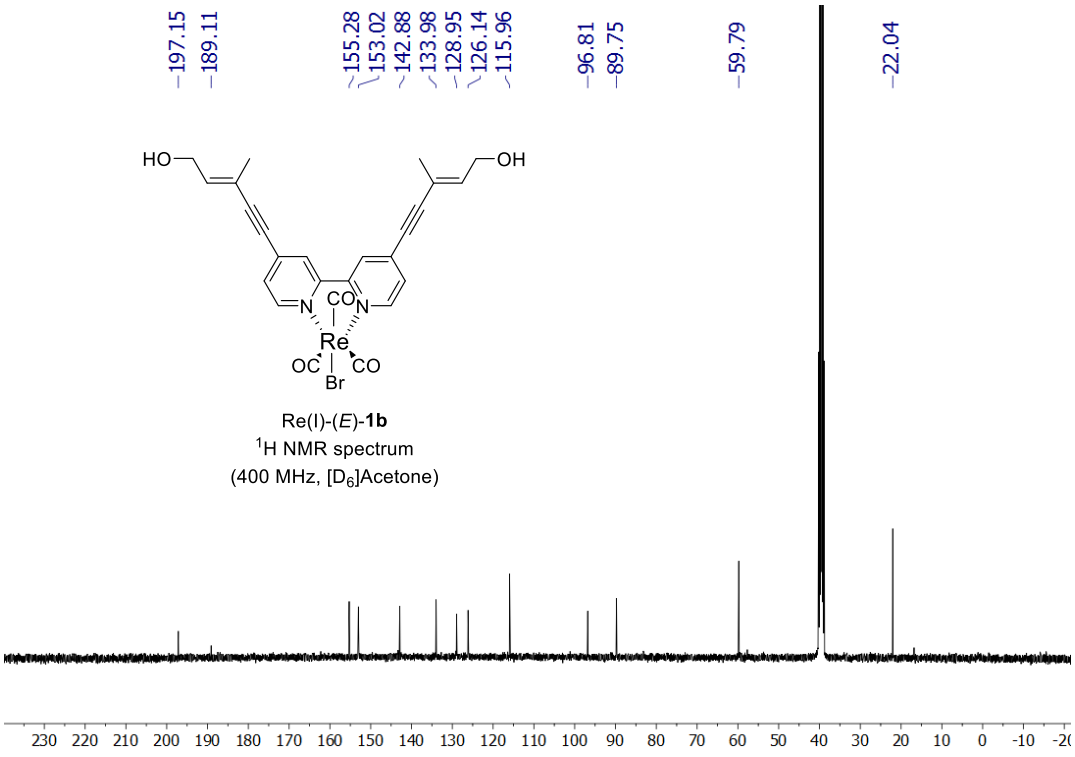

*Figure S19. Re(I)-(Z)-**1b** ^{13}C-NMR ([D$_6$]DMSO) spectra.*

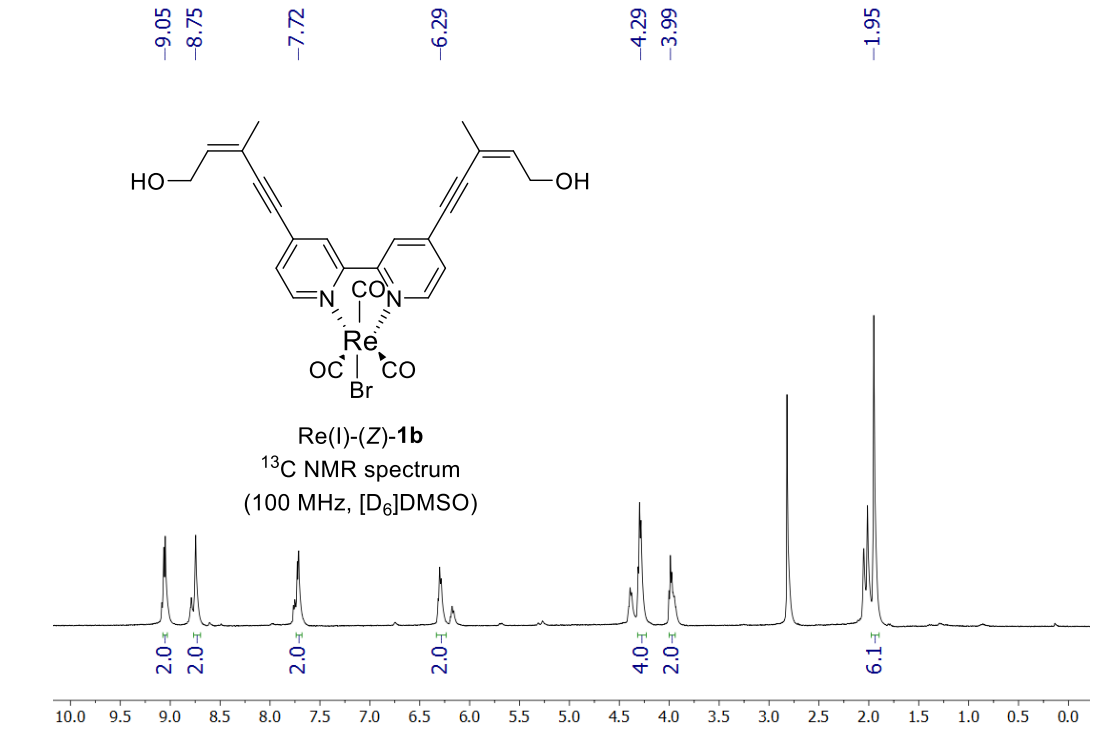

*Figure S20. Re(I)-(E)-**1b** ^{1}H-NMR ([D$_6$]Acetone) spectra.*

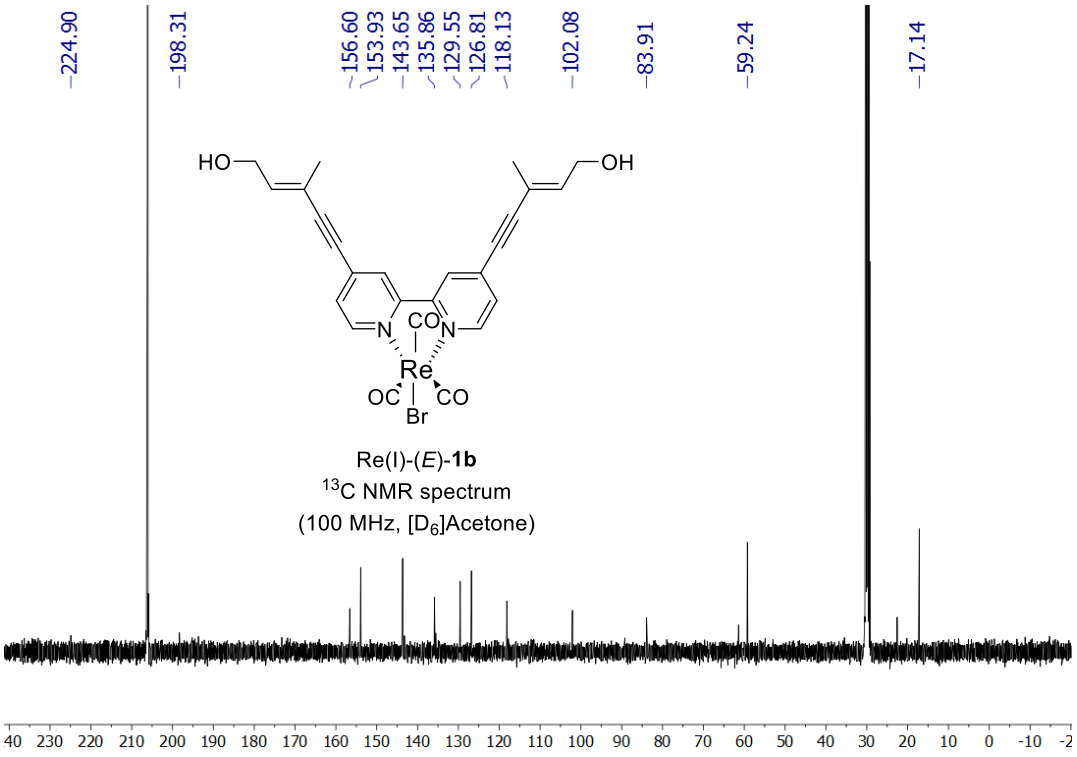

*Figure S21. Re(I)-(E)-**1b** ^{13}C-NMR ([D_6]Acetone) spectra.*

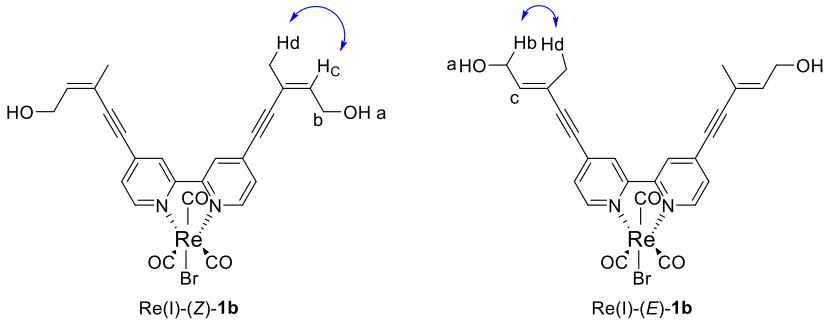

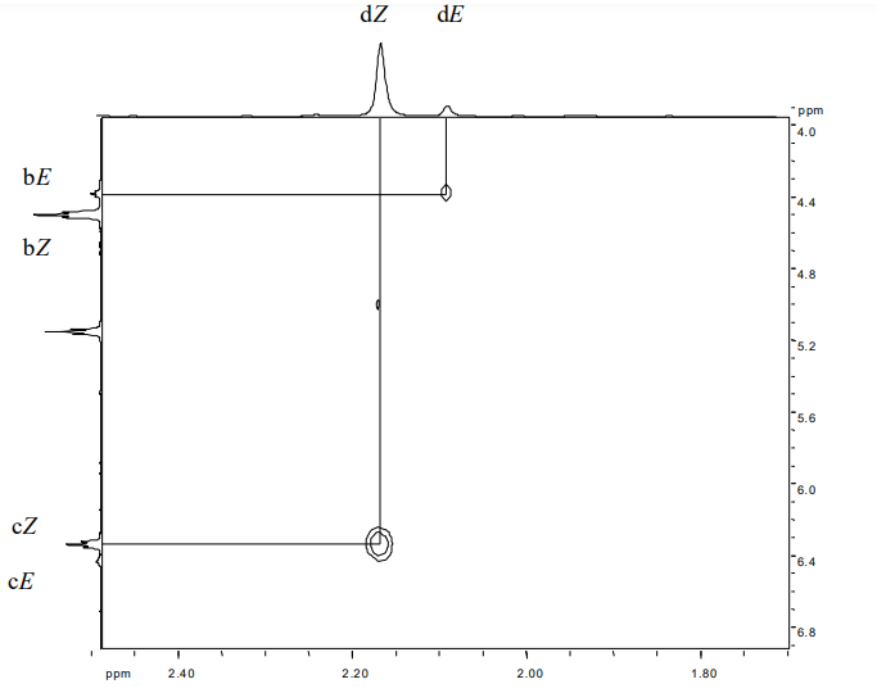

*Figure S22. Re(I)-(Z)-**1b**/Re(I)-(E)-**1b** NOESY ([D_6]DMSO).*

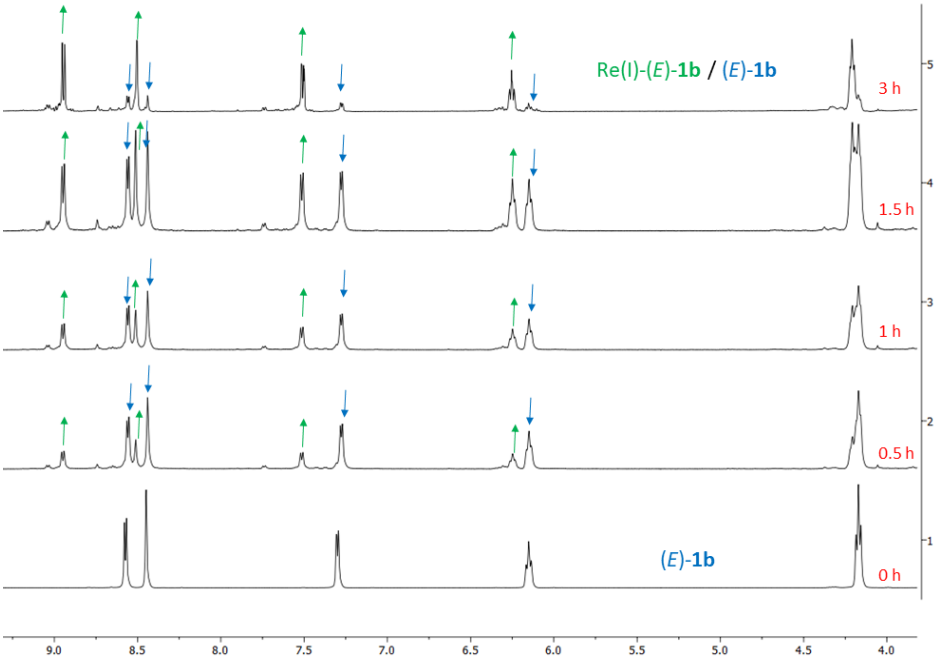

*Figure S23. Ligand exchange reaction with (E)-**1b** followed by ^{1}H-NMR ([D_8]THF) in the dark with the afore mentioned conditions. The free ligand gradually disappears, being the formation of Re(I)-(E)-**1b** complex practically complete in 3 hours.*

3.3. Complexes Re(I)-(*Z*)-1d and Re(I)-(*E*)-1d

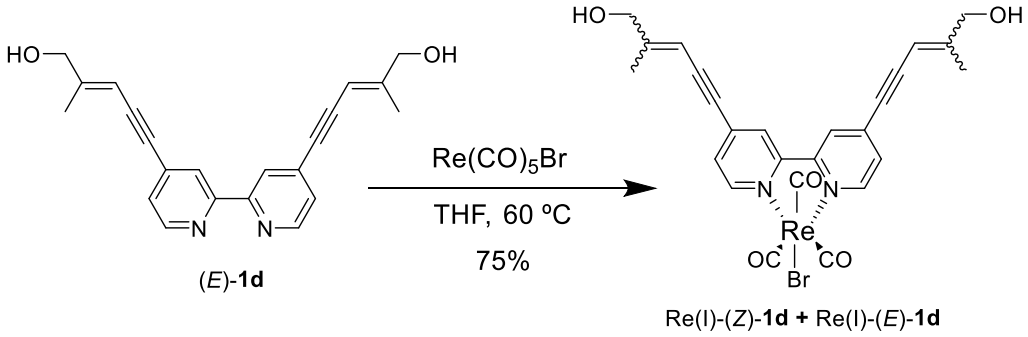

Bipyridine (*E*)-**1d** (15 mg, 0.044 mmol) and $Re(CO)_5Br$ (19.5 mg, 0.048 mmol) were placed in a Schlenk tube previously flamed and purged with Ar. Dry THF (1.3 mL) was added and the reaction mixture was stirred at 60°C for 12 h. The solvent was removed under reduced pressure and the remaining solid was purified by flash chromatography (SiO_2; 80:20 CH_2Cl_2/ CH_3CN) to give a mixture of complexes Re(I)-(*Z*)-**1d** and Re(I)-(*E*)-**1d** as an orange solid (23 mg, 75%) in a ratio 1:10 respectively.

Re(I)-(*E*)-**1d**: **^{1}H NMR** (400 MHz, CD_3OD): δ= 2.05 (s, 3H; CH_3), 4.15 (s, 2H; CH_2), 5.93 (d, *J* = 1.2 Hz, 1H; C=CH), 7.59 (dd, *J* = 5.8, 1.3 Hz, 1H; Ar-H), 8.61 (d, *J* = 1.3 Hz, 2H; Ar-H), 8.94 (d, *J* = 5.8 Hz, 2H; Ar-H). **^{13}C NMR** (100 MHz, CD_3OD): δ 17.2 (CH_3), 66.5 (CH_2), 90.5 (C), 98.3 (C), 103.2 (CH), 126.8 (CH), 129.7 (CH), 137.0 (C), 154.0 (CH), 157.1 (C), 158.4 (C), 190.0 (C), 198.1 (C). **IR** (NaCl): υ 2020 (s), 1915 (s), 1896 (s) cm^{-1}.

Re(I)-(*Z*)-**1d**: **^{1}H NMR** (400 MHz, CD_3OD): δ= 2.01 (s, 3H; CH_3), 4.45 (s, 2H; CH_2), 5.74 (d, *J* = 1.2 Hz, 1H; C=CH), 7.74 (dd, *J* = 5.8, 1.3 Hz, 1H; Ar-H), 8.75 (d, *J* = 1.3 Hz, 2H; Ar-H), 9.05 (d, *J* = 5.8 Hz, 2H; Ar-H).

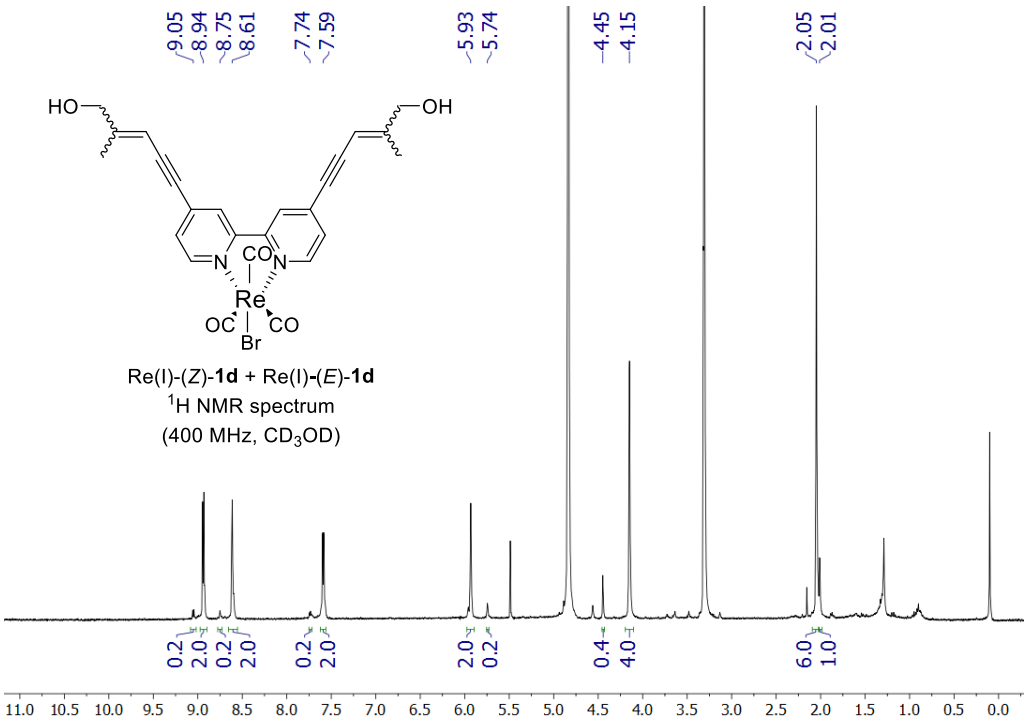

*Figure S24. Re(I)-(Z)-**1d** and Re(I)-(Z)-**1d** ^{1}H-NMR (CD_3OD) spectra.*

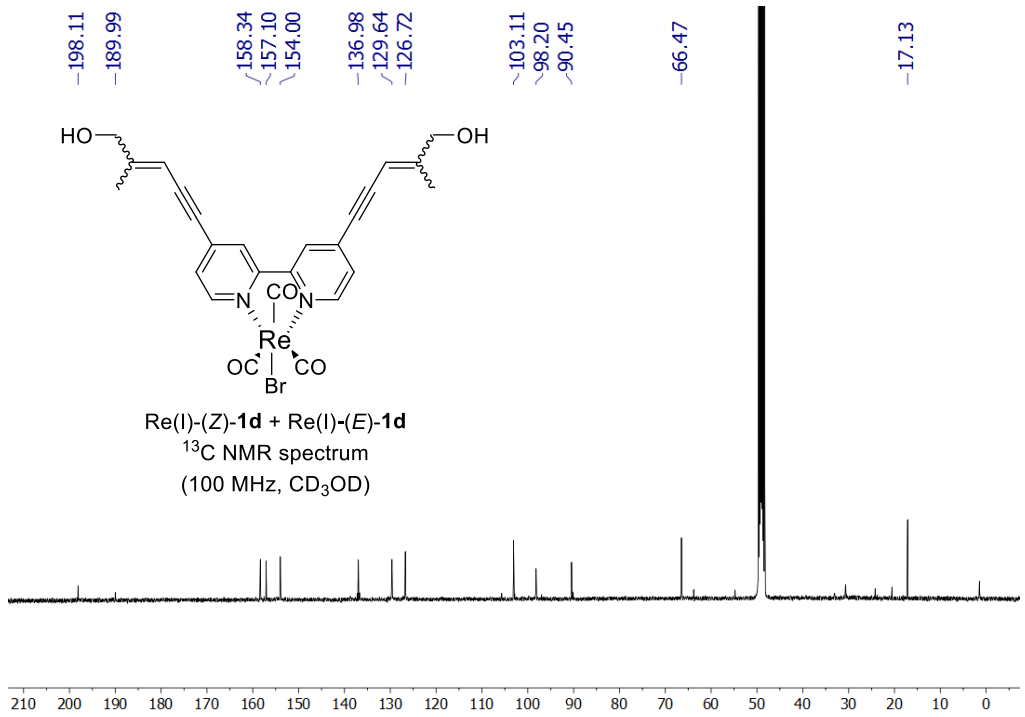

*Figure S25. Re(I)-(Z)-**1d** and Re(I)-(Z)-**1d** ^{13}C-NMR (CD_3OD) spectra.*

3.4. Complex Re(I)-(*Z*)-1e

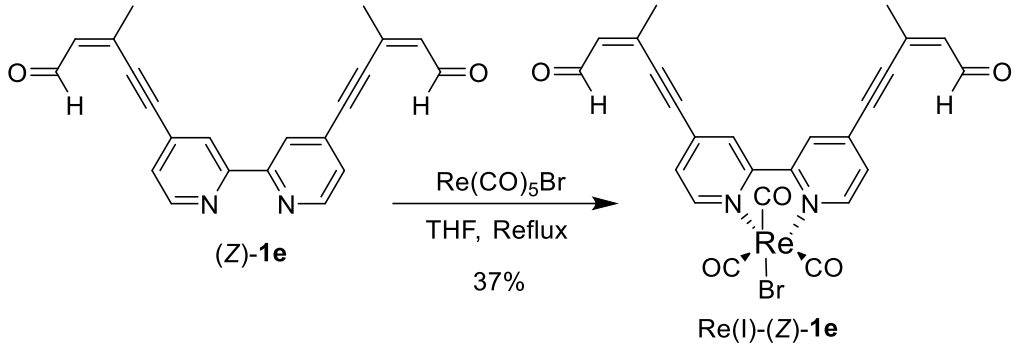

Bipyridine (*Z*)-**1e** (22 mg, 0.07 mmol) and $Re(CO)_5Br$ (29 mg, 0.07 mmol) were placed in an amber round-bottom flask previously flamed and purged with Ar. Dry THF (2.2 mL) was added and the reaction mixture was stirred and refluxed for 7 h, keeping the reaction vessel in the dark. The solvent was removed under reduced pressure and the remaining solid was purified by flash chromatography (SiO_2; 1:99 MeOH/ CH_2Cl_2) to give Re(I)-(*Z*)-**1e** as a red solid (17 mg, 37 %).

^{1}H NMR (400 MHz, [D_6]DMSO): δ= 2.29 (s br, 6H; CH_3), 6.57 (d, *J* = 8.2 Hz, 2H; C=CH), 7.92 (dd, *J* = 5.5, 1.2 Hz, 2H; Ar-H), 9.06 (s br, 2H; Ar-H), 9.09 (d, *J* = 5.5 Hz, 2H; Ar-H), 10.17 (d, *J* = 8.2 Hz, 2H; CHO). **^{13}C NMR** (100 MHz, [D_6]DMSO, 50°C): δ= 23.4 (CH3), 93.4 (C), 94.1 (C), 126.5 (CH), 129.2 (CH), 132.4 (C), 137.2 (C), 139.3 (CH), 153.0 (C), 155.1 (CH), 192.0 (CH), 192.1 (CO), 196.8 (CO). **IR** (NaCl): υ 2019 (vs), 1894 (vs) cm^{-1}. **UV/Vis** (CH_2Cl_2): λ_{max} (ε)= 435.0 nm (5259 $mol^{-1}\,dm^3\,cm^{-1}$), 318.0 nm (31805 $mol^{-1}\,dm^3\,cm^{-1}$), 289.0 nm (25948 $mol^{-1}\,dm^3\,cm^{-1}$). **MS** (FB^+): *m/z* (%): 662 (3) $[M\text{- CO}]^+$

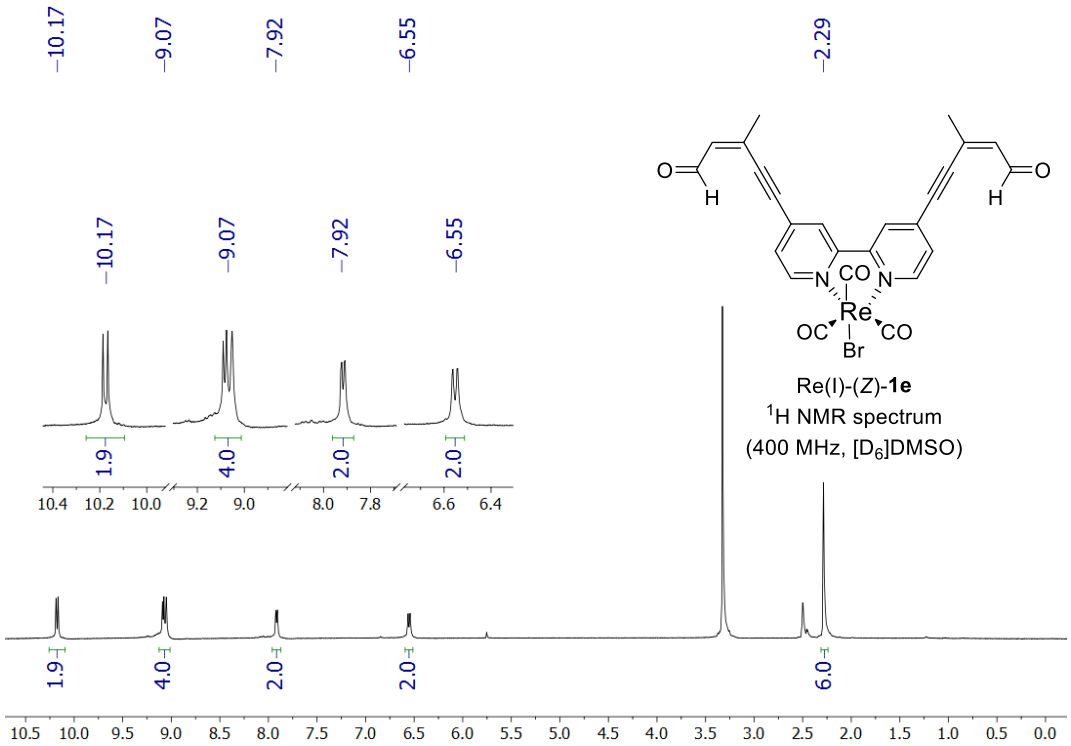

*Figure S26. Re(I)-(Z)-**1e** ^{1}H-NMR ([D_6]DMSO) spectra.*

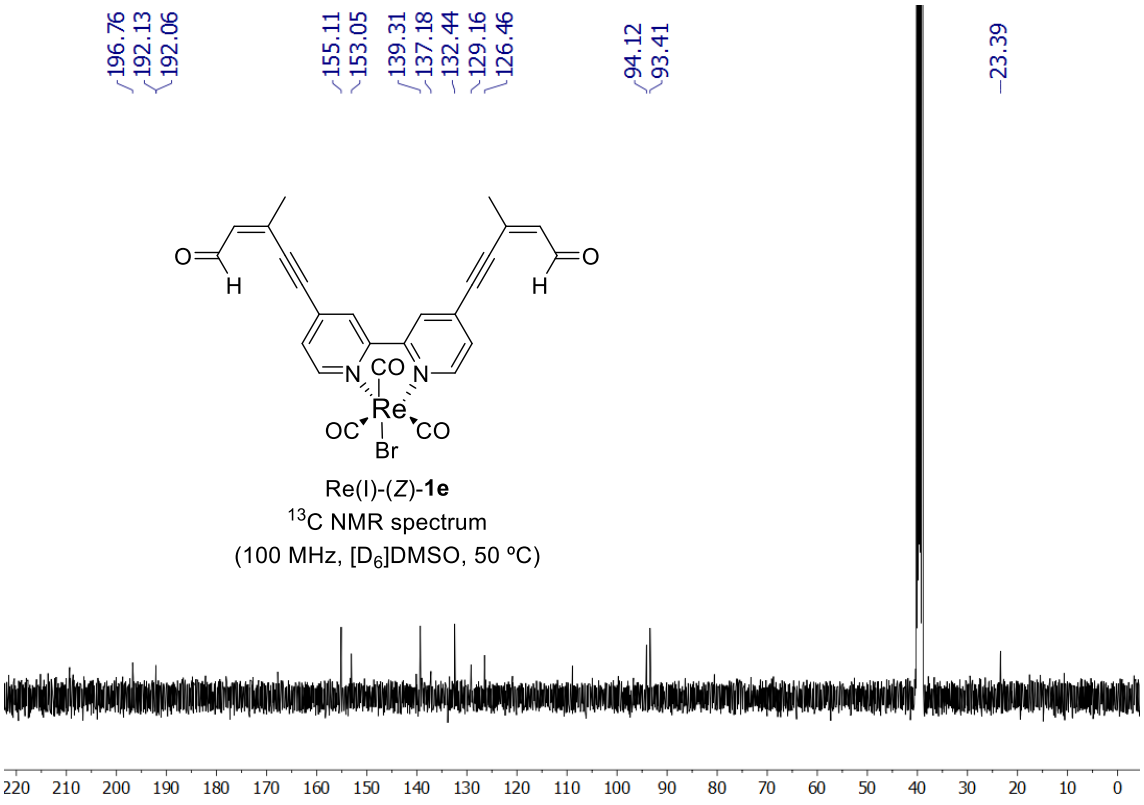

*Figure S27. Re(I)-(Z)-**1e** ^{13}C-NMR ([D$_6$]DMSO, 50 °C) spectra. It was necessary to increase the temperature to 50 °C due to the low solubility of the product. Other solvents were tested but did not improve the result.*

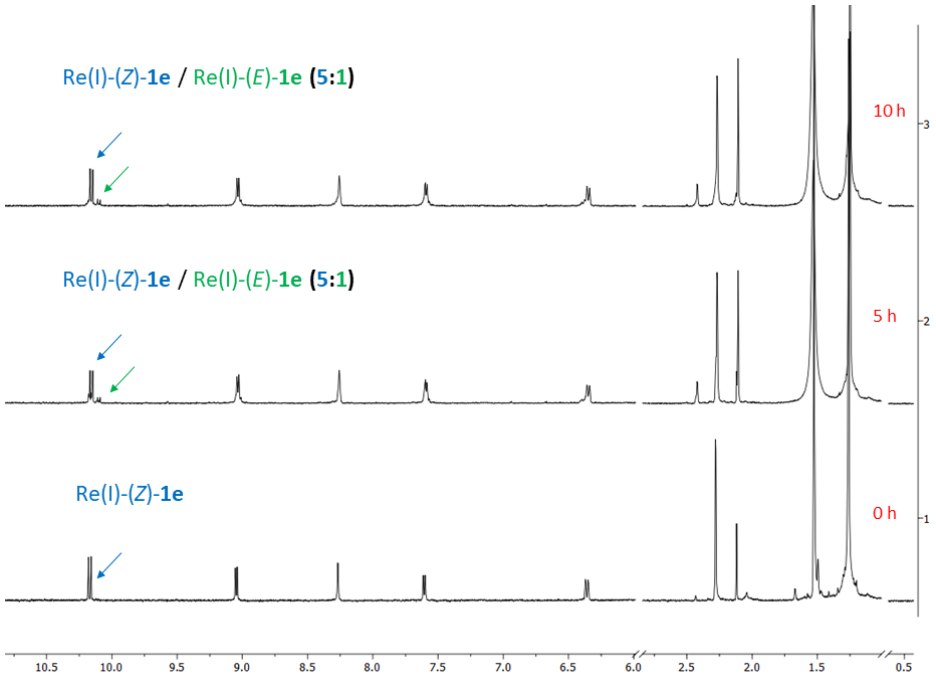

*Figure S28. Photoisomerization of Re(I)-(Z)-**1e** followed by ^{1}H-NMR (CD_2Cl_2). In the absence of light, only the Z-isomer is observed. The photostationary mixture is reached within the first 5 hours of exposure to sunlight. The blue arrow points to the aldehyde signal of Re(I)-(Z)-**1e** while the green arrow points to the aldehyde signal of Re(I)-(E)-**1e***

3.5. Complex Re(I)-(*Z*)-2b

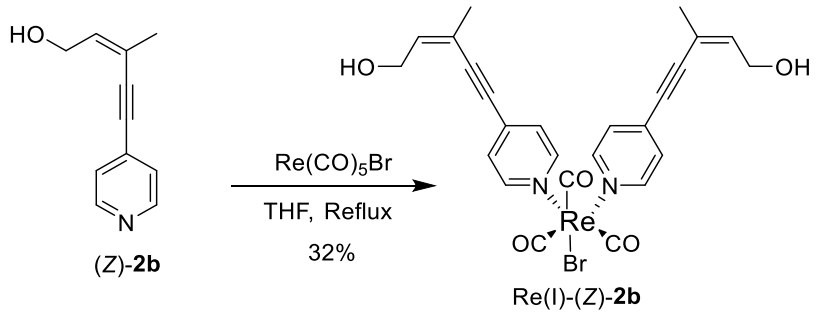

Pyridine (*Z*)-**2b** (21 mg, 0.12 mmol) and $Re(CO)_5Br$ (25 mg, 0.06 mmol) were placed in a NMR-tube with a Young valve which was then purged with Ar. THF-d^8 (1.5 mL) was added and the reaction mixture was heated at 70 °C for 16 h keeping the reaction in the dark. The solvent was removed under reduced pressure and the remaining solid was purified by flash chromatography (Al_2O_3; 10:90 CH_3CN/CH_2Cl_2) to give Re(I)-(*Z*)-**2b** as a yellow solid (14 mg, 32 %).

^{1}H NMR (400 MHz, $CDCl_3$): δ= 1.99 (s br, 6H; CH_3), 4.38 (m, 4H; CH_2), 6.08 (t, *J* = 6.7 Hz, 2H; C=CH), 7.28 (d, *J* = 6.7 Hz, 4H; Ar-H), 8.74 (d, *J* = 6.7 Hz, 4H; Ar-H). **^{13}C-NMR** (100 MHz, $CDCl_3$): δ= 22.7 (CH_3), 61.5 (CH_2), 90.2 (C), 96.5 (C), 119.4 (C), 127.5 (CH), 134.1 (C), 139.6 (CH), 154.2 (CH), 191.8 (CO), 195.0 (CO). **IR** (NaCl): υ 2019 (vs), 1898 (vs), 1876 (vs) cm^{-1}. **UV/vis** (MeOH): λ_{max} (*ε*) = 321.5 nm (sh, 20862 mol^{-1} dm^3 cm^{-1}); 303.0 nm (21902 mol^{-1} dm^3 cm^{-1}); 259.4 nm (15130 mol^{-1} dm^3 cm^{-1}). **MS** (FB^+): *m/z* (%): 696 (16) $[M]^+$.

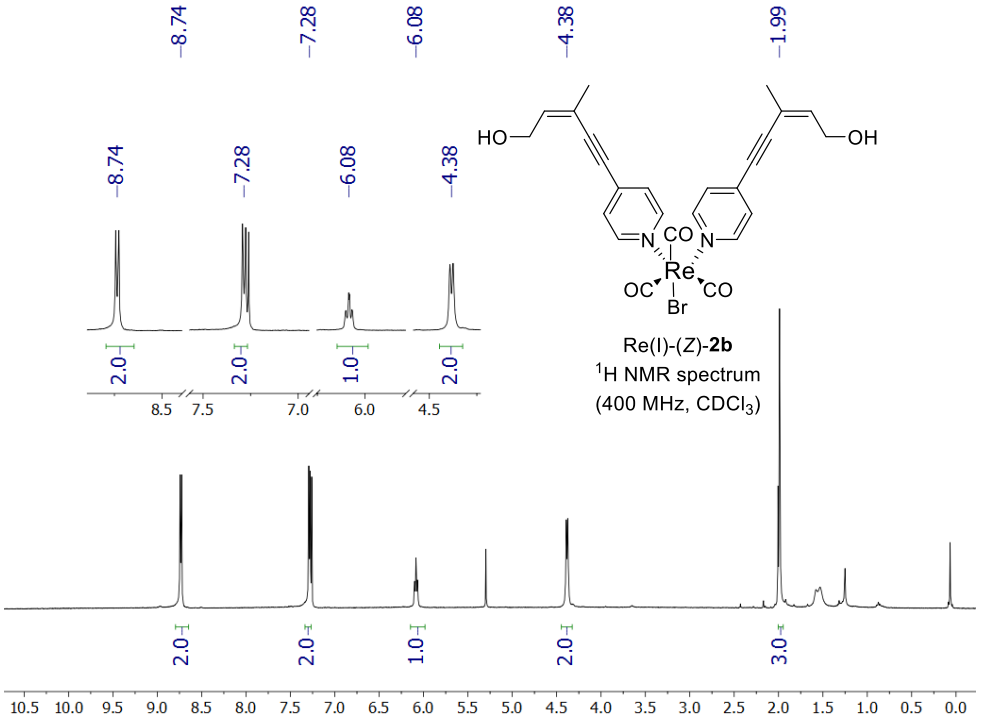

*Figure S29. Re(I)-(Z)-**2b** ^{1}H-NMR ($CDCl_3$) spectra.*

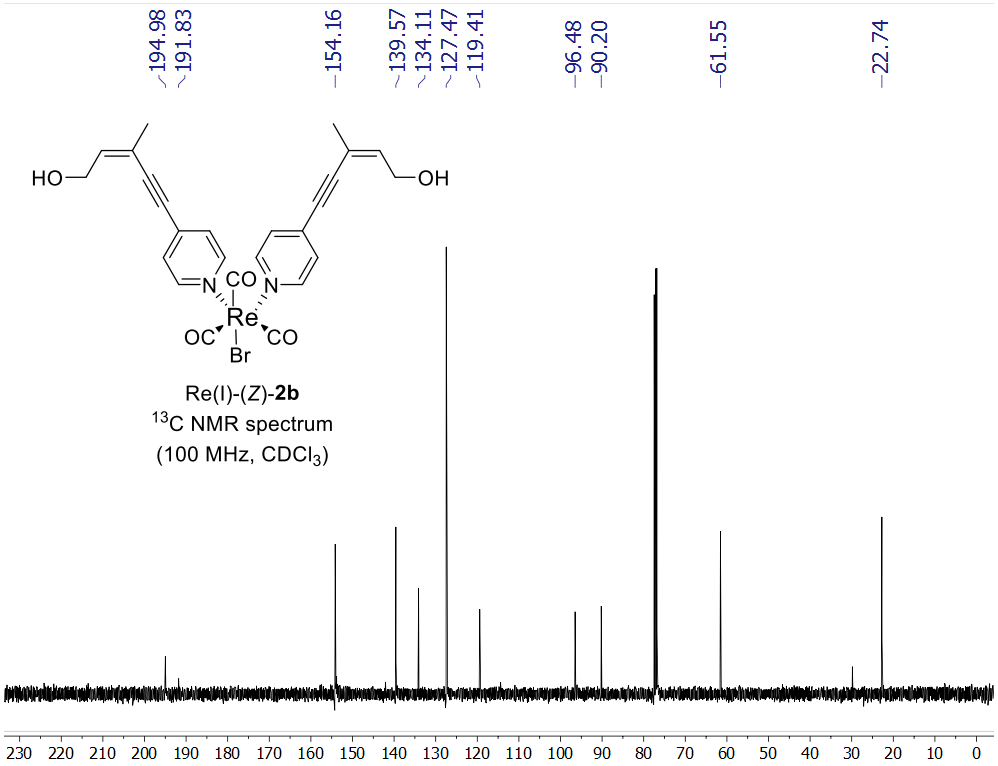

*Figure S30. Re(I)-(Z)-**2b** ^{13}C-NMR ($CDCl_3$) spectra.*

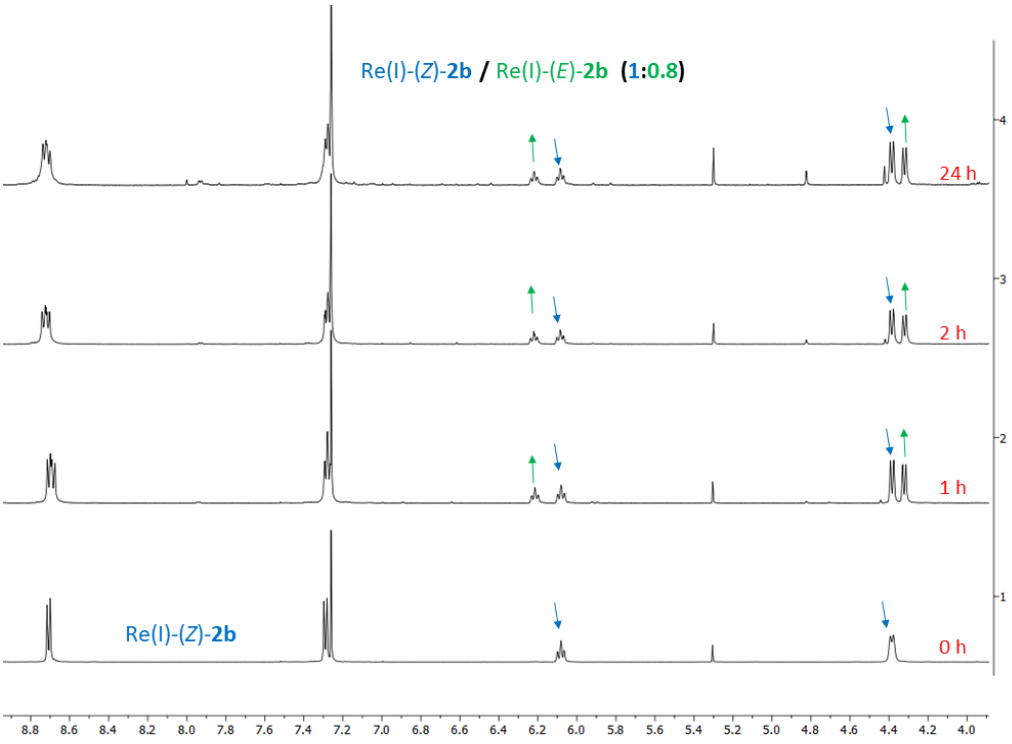

*Figure S31. Photoisomerization of Re(I)-(Z)-**2e** followed by ^{1}H-NMR (CD_3Cl). In the absence of light, only the Z-isomer is observed. The photostationary mixture is reached within the first 1 hour of exposure to sunlight. The blue arrows point some of the original signals of Re(I)-(Z)-**2e** while the green arrows point the appearance of Re(I)-(E)-**2e.***

4. Computational methodology

All the calculations performed in this work have been carried out using the Density Functional Theory[5] with the hybrid PBE0 density functional.[6] This density functional in particular, and global hybrids with 20-25% of HF exchange have been shown to provide good accuracy in describing excited states of small organic molecules and heterocyclic systems.[7] Moreover, it also provides good performance on structural parameters for organic molecules.[8] The time-dependent formulation of the Kohn-Sham equations (TDDFT) has been used for the free ligands and the Tamm-Dancoff approximation has been considered when dealing with Re complexes.[9] The latter approximation is due to TDDFT being prone to failure when dealing with large scale charge transfers and low energy singlet-triplet excitations.[10] This methodology as been paired with the double-z quality 6-31+G(d,p) basis set for the light atoms (C, N, O and H) and the LANL2DZ electron core potential (ECP) and its associated basis set for the Re atom.[11] It is worth noting that the LANL2DZ ECP is a scalar (spin-free) potential which includes scalar relativistic properties of the Re core electrons but does not include spin-orbit features (which are spin-dependent and require special ECPs with spin orbit coefficients). For this reason and the compact basis set used in this work we only expect qualitative fitting to the experiment. Full geometry optimizations were performed for all the systems in this work. Analytic second derivatives were subsequently computed and harmonic analysis used to confirm the obtained geometries represented energy minima on the potential energy surface. The optimized geometry was then subjected to 18 partial optimizations in which only one degree of freedom was held fixed (the dihedral angle associated to the isomerization process) while all other variables were allowed to optimize. On such set of globally and partially optimized geometries single point TDDFT calculations were run requesting between 15 and 50 states depending on the size of the system under investigation (50 states were included, for instance, for the Re complexes while 15 states seemed enough to reproduce the chemically relevant excitation states in free ligans A and B, as shown in Figure 7). Calculation of the total isotropic magnetic shieldings were performed at the same level of theory via the use of the Gauge Independent Atomic Orbital (GIAO) method.[12]

Simulated absorption spectra for Re(I)-**1e**

This simulated absorption spectra serves a twofold purpose. First it can be compared to the experimentally recorded spectra to showcase that the simulations are providing qualitatively accurate results for the excitation events in these complexes and, second, it helps rationalize the photostationary equilibrium in which the Z isomer is found is larger concenctration with respect to the E isomer (in a 5:1 ratio) due to the higher absorption of the latter across the UV-vis spectrum.

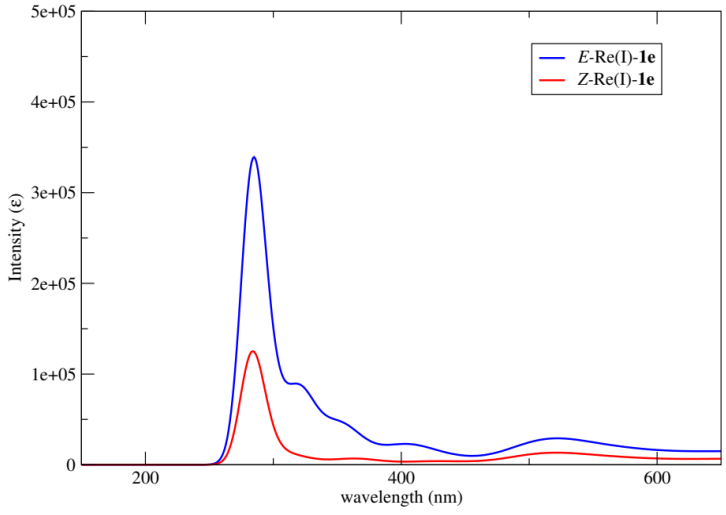

Relevant data on the excited states computed at the starting geometries

1a:

Ground to excited state transition electric dipole moments (Au):

state	X	Y	Z	Dip. S.	Osc.
1	0.0000	0.0000	-0.0000	0.0000	0.0000
2	0.0000	0.0000	-0.0000	0.0000	0.0000
3	0.0000	-0.0000	0.0000	0.0000	0.0000
4	0.0000	-0.0000	0.0000	0.0000	0.0000
5	0.0000	-0.0000	0.0000	0.0000	0.0000
6	-0.0000	-0.0000	0.0000	0.0000	0.0000
7	-0.0000	0.0000	0.0000	0.0000	0.0000
8	0.0000	-0.0000	0.0000	0.0000	0.0000
9	0.0000	-0.0000	0.0000	0.0000	0.0000
10	0.0000	-0.0000	0.0000	0.0000	0.0000
11	0.0000	-0.0000	0.0000	0.0000	0.0000
12	0.0000	-0.0000	-0.0000	0.0000	0.0000
13	-0.0000	0.0000	-0.0000	0.0000	0.0000
14	3.6618	0.4071	0.1817	13.6078	1.3682
15	0.0001	-0.0001	0.0000	0.0000	0.0000

Ground to excited state transition velocity dipole moments (Au):

state	X	Y	Z	Dip. S.	Osc.
1	-0.0000	-0.0000	0.0000	0.0000	0.0000
2	0.0000	-0.0000	0.0000	0.0000	0.0000
3	-0.0000	0.0000	0.0000	0.0000	0.0000
4	-0.0000	0.0000	0.0000	0.0000	0.0000
5	-0.0000	0.0000	0.0000	0.0000	0.0000
6	-0.0000	-0.0000	-0.0000	0.0000	0.0000
7	-0.0000	-0.0000	0.0000	0.0000	0.0000
8	-0.0000	0.0000	0.0000	0.0000	0.0000
9	-0.0000	0.0000	0.0000	0.0000	0.0000
10	-0.0000	0.0000	-0.0000	0.0000	0.0000
11	-0.0000	-0.0000	0.0000	0.0000	0.0000
12	0.0000	0.0000	-0.0000	0.0000	0.0000
13	0.0000	-0.0000	0.0000	0.0000	0.0000
14	-0.5430	-0.0616	-0.0264	0.2993	1.3230
15	-0.0000	0.0000	-0.0000	0.0000	0.0000

Ground to excited state transition magnetic dipole moments (Au):

state	X	Y	Z
1	-0.0000	0.0000	0.0000
2	-0.0000	0.0000	0.0000
3	-0.0000	-0.0001	-0.0000
4	-0.0000	-0.0001	-0.0000
5	-0.0000	-0.0001	-0.0000
6	0.0000	-0.0000	-0.0000
7	0.0000	-0.0000	0.0000
8	-0.0000	-0.0000	-0.0000
9	-0.0000	-0.0001	-0.0000
10	-0.0000	-0.0000	-0.0000
11	-0.0000	-0.0000	0.0000
12	-0.0000	0.0000	-0.0000
13	0.0000	0.0000	0.0000
14	0.1111	0.1069	-2.5825
15	-0.0000	-0.0001	-0.0001

Re-1a:

Ground to excited state transition electric dipole moments (Au):

state	X	Y	Z	Dip. S.	Osc.
1	0.0000	0.0000	-0.0000	0.0000	0.0000
2	-0.0000	0.0000	-0.0000	0.0000	0.0000
3	0.3215	-0.1664	-0.0043	0.1311	0.0092
4	0.4933	1.0224	-0.0659	1.2930	0.0940
5	0.0000	0.0000	0.0000	0.0000	0.0000
6	-0.0000	0.0000	-0.0000	0.0000	0.0000
7	-0.0000	-0.0000	-0.0000	0.0000	0.0000
8	0.0000	0.0000	0.0000	0.0000	0.0000
9	0.0351	0.0674	0.0024	0.0058	0.0005
10	-0.0001	0.0001	-0.0000	0.0000	0.0000
11	0.0002	0.0000	-0.0000	0.0000	0.0000
12	0.0002	-0.0001	0.0000	0.0000	0.0000
13	0.0001	-0.0000	0.0000	0.0000	0.0000
14	-0.0000	-0.0000	0.0000	0.0000	0.0000
15	-0.5183	-0.7641	0.2155	0.8989	0.0850

Ground to excited state transition velocity dipole moments (Au):

state	X	Y	Z	Dip. S.	Osc.
1	-0.0000	-0.0000	0.0000	0.0000	0.0000
2	0.0000	-0.0000	0.0000	0.0000	0.0000
3	0.0022	0.0028	-0.0003	0.0000	0.0001
4	-0.0228	-0.0276	-0.0082	0.0014	0.0083
5	-0.0000	-0.0000	0.0000	0.0000	0.0000
6	0.0000	-0.0000	0.0000	0.0000	0.0000
7	0.0000	0.0000	-0.0000	0.0000	0.0000
8	-0.0000	-0.0000	0.0000	0.0000	0.0000
9	-0.0021	-0.0038	-0.0021	0.0000	0.0001
10	0.0000	-0.0000	0.0000	0.0000	0.0000
11	-0.0000	-0.0000	0.0000	0.0000	0.0000
12	-0.0000	0.0000	-0.0000	0.0000	0.0000
13	-0.0000	0.0000	-0.0000	0.0000	0.0000
14	0.0000	0.0000	-0.0000	0.0000	0.0000
15	0.0459	0.0511	0.0047	0.0047	0.0223

Ground to excited state transition magnetic dipole moments (Au):

state	X	Y	Z
1	0.0000	-0.0000	0.0000
2	-0.0000	-0.0000	0.0000
3	0.0378	0.1080	-0.2555
4	0.0269	0.0015	0.1597
5	0.0000	-0.0000	0.0000
6	-0.0000	-0.0000	-0.0000
7	-0.0000	0.0000	-0.0000
8	0.0000	-0.0000	0.0000
9	-0.1801	0.0703	0.0184
10	-0.0001	-0.0000	0.0000
11	0.0002	-0.0000	0.0002
12	0.0001	0.0000	-0.0000
13	0.0001	0.0000	-0.0000
14	-0.0000	0.0000	-0.0000
15	0.2959	-0.1493	-0.2208

1e:

Ground to excited state transition electric dipole moments (Au):

state	X	Y	Z	Dip. S.	Osc.
1	0.0000	0.0000	0.0000	0.0000	0.0000
2	0.0000	-0.0000	0.0000	0.0000	0.0000
3	-0.0000	-0.0000	0.0000	0.0000	0.0000
4	0.0000	-0.0000	-0.0000	0.0000	0.0000
5	0.0000	-0.0000	0.0000	0.0000	0.0000
6	-0.0000	0.0000	-0.0000	0.0000	0.0000
7	0.0082	-0.0035	-0.0546	0.0031	0.0003
8	-0.0006	-0.0423	0.0044	0.0018	0.0002
9	-0.0000	0.0000	-0.0000	0.0000	0.0000
10	-0.0000	-0.0000	0.0000	0.0000	0.0000
11	0.0000	-0.0000	-0.0000	0.0000	0.0000
12	0.0000	-0.0000	0.0000	0.0000	0.0000
13	0.0000	0.0000	0.0000	0.0000	0.0000
14	3.4372	-0.0000	0.0086	11.8143	1.2401
15	-0.0001	-1.7878	-0.0000	3.1961	0.3442
16	0.0000	-0.0000	-0.0000	0.0000	0.0000
17	0.0000	0.0000	0.0000	0.0000	0.0000
18	0.0000	-0.0000	0.0000	0.0000	0.0000
19	0.0002	0.0204	0.0000	0.0004	0.0000
20	0.0933	-0.0001	0.1565	0.0332	0.0037
21	-1.0506	-0.0002	0.3110	1.2006	0.1387
22	0.0026	-0.0465	-0.0005	0.0022	0.0003
23	-0.3850	0.0002	0.1064	0.1595	0.0186
24	-0.0000	-0.2232	-0.0000	0.0498	0.0059
25	-0.0000	0.0000	0.0000	0.0000	0.0000
26	0.0000	0.0000	-0.0000	0.0000	0.0000
27	0.0000	0.0000	-0.0000	0.0000	0.0000
28	0.0000	-0.0000	-0.0000	0.0000	0.0000
29	-0.0000	-0.0000	0.0000	0.0000	0.0000
30	-0.0000	0.0000	0.0000	0.0000	0.0000

Ground to excited state transition velocity dipole moments (Au):

state	X	Y	Z	Dip. S.	Osc.
1	-0.0000	0.0000	-0.0000	0.0000	0.0000
2	0.0000	-0.0000	-0.0000	0.0000	0.0000
3	0.0000	-0.0000	0.0000	0.0000	0.0000
4	-0.0000	0.0000	0.0000	0.0000	0.0000
5	-0.0000	0.0000	-0.0000	0.0000	0.0000
6	0.0000	-0.0000	-0.0000	0.0000	0.0000

7	-0.0028	0.0002	0.0005	0.0000	0.0000
8	0.0002	0.0025	-0.0000	0.0000	0.0000
9	0.0000	-0.0000	0.0000	0.0000	0.0000
10	0.0000	-0.0000	0.0000	0.0000	0.0000
11	-0.0000	0.0000	0.0000	0.0000	0.0000
12	-0.0000	0.0000	0.0000	0.0000	0.0000
13	-0.0000	-0.0000	-0.0000	0.0000	0.0000
14	-0.5285	0.0000	-0.0032	0.2793	1.1826
15	0.0000	0.2856	0.0000	0.0816	0.3366
16	0.0000	0.0000	0.0000	0.0000	0.0000
17	0.0000	-0.0000	0.0000	0.0000	0.0000
18	-0.0000	0.0000	-0.0000	0.0000	0.0000
19	-0.0000	-0.0083	-0.0000	0.0001	0.0003
20	-0.0189	0.0000	-0.0378	0.0018	0.0071
21	0.1784	0.0000	-0.0536	0.0347	0.1334
22	-0.0004	0.0116	0.0001	0.0001	0.0005
23	0.0644	-0.0000	-0.0272	0.0049	0.0186
24	0.0000	0.0398	0.0000	0.0016	0.0059
25	0.0000	-0.0000	-0.0000	0.0000	0.0000
26	0.0000	-0.0000	0.0000	0.0000	0.0000
27	0.0000	-0.0000	0.0000	0.0000	0.0000
28	-0.0000	0.0000	0.0000	0.0000	0.0000
29	0.0000	0.0000	-0.0000	0.0000	0.0000
30	0.0000	-0.0000	-0.0000	0.0000	0.0000

Ground to excited state transition magnetic dipole moments (Au):

state	X	Y	Z
1	-0.0000	0.0000	-0.0000
2	-0.0000	0.0000	0.0000
3	0.0000	0.0000	0.0000
4	-0.0000	0.0000	-0.0000
5	-0.0000	-0.0000	-0.0000
6	0.0000	0.0000	0.0000
7	1.0472	0.0105	-0.3059
8	-0.0844	0.1305	0.0246
9	0.0000	-0.0000	-0.0000
10	0.0000	0.0000	-0.0000
11	0.0000	-0.0000	0.0000
12	0.0000	0.0000	0.0000
13	-0.0000	0.0000	0.0000
14	-0.3415	-0.0002	1.2609
15	-0.0000	-0.5289	0.0000

16	-0.0000	0.0000	0.0000
17	-0.0000	0.0000	0.0000
18	0.0000	0.0000	0.0000
19	-0.0000	-0.2679	0.0001
20	-1.0343	-0.0000	0.4134
21	-0.4056	-0.0000	-0.2752
22	-0.0013	0.1736	0.0016
23	0.2663	0.0009	-0.2372
24	0.0000	0.2151	-0.0000
25	-0.0000	0.0000	0.0000
26	0.0000	-0.0000	-0.0000
27	0.0000	-0.0000	0.0000
28	0.0000	-0.0000	-0.0000
29	-0.0000	0.0000	-0.0000
30	0.0000	0.0000	0.0000

Re-1e:

Ground to excited state transition electric dipole moments (Au):

state	X	Y	Z	Dip. S.	Osc.
1	0.0000	0.0000	0.0000	0.0000	0.0000
2	0.0000	0.0000	-0.0000	0.0000	0.0000
3	0.4028	0.0001	-0.0000	0.1622	0.0105
4	0.0000	-0.0000	0.0000	0.0000	0.0000
5	0.0000	-0.0000	0.0000	0.0000	0.0000
6	-0.0000	1.0533	-0.0120	1.1095	0.0754
7	0.0000	0.0000	0.0000	0.0000	0.0000
8	-0.0000	-0.0000	-0.0000	0.0000	0.0000
9	0.0000	-0.0000	0.0000	0.0000	0.0000
10	-0.0000	-0.0000	-0.0000	0.0000	0.0000
11	0.0000	0.0816	-0.0026	0.0067	0.0005
12	-0.0000	-0.0000	0.0000	0.0000	0.0000
13	0.0000	0.0000	-0.0000	0.0000	0.0000
14	-0.0787	0.0005	-0.0004	0.0062	0.0005
15	0.0007	0.0555	-0.0525	0.0058	0.0005
16	0.0000	0.0000	0.0000	0.0000	0.0000
17	0.0002	0.3785	0.1322	0.1608	0.0139
18	0.9889	-0.0000	-0.0000	0.9779	0.0856
19	0.0000	0.0000	-0.0000	0.0000	0.0000
20	-0.0000	-0.0000	-0.0000	0.0000	0.0000
21	0.9579	-0.0007	0.0000	0.9176	0.0840
22	-0.0000	-0.0000	0.0000	0.0000	0.0000
23	-0.0022	1.8274	-0.0758	3.3450	0.3077
24	0.2070	0.0226	-0.0010	0.0434	0.0040
25	0.0001	0.2566	-0.1179	0.0797	0.0074
26	0.0000	0.0000	-0.0000	0.0000	0.0000
27	0.0000	0.0000	0.0000	0.0000	0.0000
28	-0.0000	-0.0000	-0.0000	0.0000	0.0000
29	0.0000	0.0000	-0.0000	0.0000	0.0000
30	0.0000	0.0000	0.0000	0.0000	0.0000

Ground to excited state transition velocity dipole moments (Au):

state	X	Y	Z	Dip. S.	Osc.
1	-0.0000	-0.0000	-0.0000	0.0000	0.0000
2	-0.0000	-0.0000	-0.0000	0.0000	0.0000
3	0.0044	-0.0000	-0.0000	0.0000	0.0001
4	-0.0000	-0.0000	-0.0000	0.0000	0.0000
5	0.0000	0.0000	0.0000	0.0000	0.0000
6	-0.0000	-0.0144	-0.0050	0.0002	0.0015

7	-0.0000	0.0000	-0.0000	0.0000	0.0000
8	0.0000	0.0000	0.0000	0.0000	0.0000
9	0.0000	0.0000	-0.0000	0.0000	0.0000
10	0.0000	0.0000	0.0000	0.0000	0.0000
11	-0.0000	-0.0030	-0.0031	0.0000	0.0001
12	0.0000	0.0000	-0.0000	0.0000	0.0000
13	-0.0000	-0.0000	0.0000	0.0000	0.0000
14	0.0050	-0.0000	0.0001	0.0000	0.0001
15	-0.0000	-0.0042	0.0119	0.0002	0.0008
16	0.0000	0.0000	0.0000	0.0000	0.0000
17	-0.0000	-0.0175	0.0079	0.0004	0.0019
18	-0.0535	0.0000	-0.0000	0.0029	0.0145
19	-0.0000	-0.0000	0.0000	0.0000	0.0000
20	0.0000	-0.0000	-0.0000	0.0000	0.0000
21	-0.0777	0.0000	-0.0000	0.0060	0.0293
22	0.0000	0.0000	-0.0000	0.0000	0.0000
23	0.0002	-0.1015	0.0079	0.0104	0.0500
24	-0.0191	-0.0013	0.0001	0.0004	0.0018
25	-0.0000	0.0011	0.0056	0.0000	0.0002
26	0.0000	0.0000	0.0000	0.0000	0.0000
27	-0.0000	0.0000	-0.0000	0.0000	0.0000
28	0.0000	0.0000	0.0000	0.0000	0.0000
29	-0.0000	-0.0000	-0.0000	0.0000	0.0000
30	-0.0000	-0.0000	-0.0000	0.0000	0.0000

Ground to excited state transition magnetic dipole moments (Au):

state	X	Y	Z
1	0.0000	0.0000	-0.0000
2	0.0000	-0.0000	0.0000
3	0.0000	0.0897	-0.0891
4	0.0000	0.0000	-0.0000
5	-0.0000	-0.0000	0.0000
6	0.0815	-0.0000	0.0000
7	-0.0000	0.0000	0.0000
8	0.0000	-0.0000	0.0000
9	0.0000	0.0000	-0.0000
10	0.0000	-0.0000	0.0000
11	-0.2191	0.0000	-0.0000
12	0.0000	-0.0000	0.0000
13	-0.0000	0.0000	0.0000
14	-0.0076	-0.0129	-0.0589
15	-0.9018	0.0001	0.0007

16	0.0000	-0.0000	0.0000
17	0.0181	-0.0000	-0.0000
18	-0.0000	-0.0125	-0.1373
19	-0.0000	-0.0000	-0.0000
20	-0.0000	-0.0000	0.0000
21	0.0001	0.0413	-0.3680
22	0.0000	0.0000	-0.0000
23	-0.3842	-0.0026	0.0030
24	-0.0047	0.2163	-0.2532
25	0.0203	-0.0000	0.0000
26	0.0000	-0.0000	0.0000
27	0.0000	0.0000	-0.0000
28	-0.0000	-0.0000	0.0000
29	-0.0000	-0.0000	0.0000
30	-0.0000	0.0000	-0.0000

A:

Ground to excited state transition electric dipole moments (Au):

state	X	Y	Z	Dip. S.	Osc.
1	0.0000	0.0000	0.0000	0.0000	0.0000
2	-3.5235	-0.1448	-0.0001	12.4360	0.7921
3	-0.0000	-0.0000	-0.0000	0.0000	0.0000
4	0.0000	0.0000	0.0000	0.0000	0.0000
5	-0.0000	-0.0000	0.0000	0.0000	0.0000
6	-0.0000	-0.0000	-0.0000	0.0000	0.0000
7	0.0000	0.0000	0.0001	0.0000	0.0000
8	0.0000	-0.0000	0.0000	0.0000	0.0000
9	-0.0000	0.0000	0.0000	0.0000	0.0000
10	0.0000	0.0000	0.0000	0.0000	0.0000
11	0.0000	0.0000	0.0000	0.0000	0.0000
12	-0.0421	0.1714	0.0000	0.0311	0.0028
13	-0.0000	-0.0000	0.0000	0.0000	0.0000
14	0.0000	0.0000	-0.0000	0.0000	0.0000
15	0.0001	0.0000	-0.0001	0.0000	0.0000

Ground to excited state transition velocity dipole moments (Au):

state	X	Y	Z	Dip. S.	Osc.
1	-0.0000	-0.0000	0.0000	0.0000	0.0000
2	0.3401	0.0151	0.0001	0.1159	0.8088
3	0.0000	0.0000	-0.0000	0.0000	0.0000
4	-0.0000	-0.0000	0.0000	0.0000	0.0000
5	-0.0000	-0.0000	0.0000	0.0000	0.0000
6	0.0000	0.0000	-0.0000	0.0000	0.0000
7	-0.0000	-0.0000	-0.0000	0.0000	0.0000
8	-0.0000	-0.0000	0.0000	0.0000	0.0000
9	-0.0000	-0.0000	0.0000	0.0000	0.0000
10	-0.0000	-0.0000	0.0000	0.0000	0.0000
11	-0.0000	-0.0000	0.0000	0.0000	0.0000
12	0.0040	-0.0156	0.0000	0.0003	0.0013
13	0.0000	-0.0000	-0.0000	0.0000	0.0000
14	-0.0000	-0.0000	0.0000	0.0000	0.0000
15	-0.0000	-0.0000	0.0000	0.0000	0.0000

Ground to excited state transition magnetic dipole moments (Au):

state	X	Y	Z
1	-0.0000	0.0000	-0.0000
2	0.0327	-0.1402	0.0000
3	0.0000	-0.0000	0.0000
4	-0.0000	0.0000	-0.0000
5	-0.0000	0.0000	-0.0000
6	0.0000	-0.0000	0.0000
7	-0.0001	0.0002	-0.0004
8	-0.0000	0.0000	-0.0000
9	-0.0000	0.0000	-0.0000
10	-0.0000	0.0001	-0.0001
11	-0.0000	0.0000	-0.0000
12	-0.0065	-0.0036	0.0000
13	0.0000	-0.0000	0.0000
14	0.0000	0.0000	0.0000
15	0.0000	0.0004	-0.0000

B:

Ground to excited state transition electric dipole moments (Au):

state	X	Y	Z	Dip. S.	Osc.
1	-0.0000	0.0000	0.0000	0.0000	0.0000
2	-0.0000	-0.0000	-0.0000	0.0000	0.0000
3	0.0000	0.0000	-0.0000	0.0000	0.0000
4	4.7525	-0.0377	-0.1000	22.5981	1.8395
5	0.0000	0.0000	-0.0000	0.0000	0.0000
6	-0.0000	-0.0000	0.0000	0.0000	0.0000
7	0.0000	0.0000	0.0000	0.0000	0.0000
8	0.0000	-0.0000	-0.0000	0.0000	0.0000
9	0.0000	-0.0000	-0.0000	0.0000	0.0000
10	-0.0000	-0.0000	-0.0000	0.0000	0.0000
11	-0.7759	-0.1134	0.0674	0.6195	0.0631
12	1.6867	0.3028	-0.0753	2.9423	0.3015
13	0.0453	0.5430	-0.0985	0.3065	0.0322
14	0.0000	-0.0000	-0.0000	0.0000	0.0000
15	0.0374	0.0976	-0.0173	0.0112	0.0012

Ground to excited state transition velocity dipole moments (Au):

state	X	Y	Z	Dip. S.	Osc.
1	-0.0000	-0.0000	0.0000	0.0000	0.0000
2	0.0000	-0.0000	-0.0000	0.0000	0.0000
3	-0.0000	0.0000	0.0000	0.0000	0.0000
4	-0.5690	0.0039	0.0119	0.3239	1.7687
5	-0.0000	-0.0000	0.0000	0.0000	0.0000
6	0.0000	-0.0000	-0.0000	0.0000	0.0000
7	-0.0000	0.0000	-0.0000	0.0000	0.0000
8	0.0000	0.0000	0.0000	0.0000	0.0000
9	-0.0000	-0.0000	0.0000	0.0000	0.0000
10	0.0000	0.0000	-0.0000	0.0000	0.0000
11	0.1152	0.0188	-0.0083	0.0137	0.0597
12	-0.2575	-0.0453	0.0123	0.0685	0.2970
13	-0.0078	-0.0931	0.0168	0.0090	0.0382
14	-0.0000	0.0000	0.0000	0.0000	0.0000
15	-0.0058	-0.0145	0.0029	0.0003	0.0011

Ground to excited state transition magnetic dipole moments (Au):

state	X	Y	Z
1	0.0000	0.0000	-0.0000
2	-0.0000	-0.0000	0.0000
3	0.0000	0.0000	-0.0000
4	0.0164	0.0611	0.9366
5	0.0000	0.0000	-0.0000
6	-0.0000	-0.0000	0.0000
7	-0.0000	-0.0000	0.0000
8	0.0000	0.0000	-0.0000
9	0.0000	-0.0000	-0.0000
10	-0.0000	-0.0000	0.0000
11	-0.2626	-0.3357	-0.3440
12	-0.0919	-0.1182	0.8714
13	0.0295	-0.1611	-0.8552
14	0.0000	-0.0000	-0.0000
15	-0.0258	-0.1357	-0.6449

Full numeric for the one-dimensional plots provided in Figures 4, 5 and 7.

Raw data for the 20 lowest lying states of the systems included in this work can be found below

1a:

S0 SCF (a.u.)	-1658.04586	-1658.04506	-1658.04295	-1658.03959	-1658.03503	-1658.02929	-1658.02252	-1658.01485	-1658.00616	-1657.99634	-1658.0085	-1658.01697	-1658.02442	-1658.031	-1658.03644	-1658.0407	-1658.04372	-1658.04548	-1658.04583
T1 SCF (a.u.)	-1657.9301854	-1657.92993	-1657.9295	-1657.93005	-1657.9315	-1657.93274	-1657.9325	-1657.93172	-1657.93006	-1657.92693	-1657.93043	-1657.9319	-1657.93231	-1657.93223	-1657.93074	-1657.92987	-1657.92989	-1657.93025	-1657.93031
Osc. Str.	90	100	110	120	130	140	150	160	170	180	190	200	210	220	230	240	250	260	270
S0	0.000	0.022	0.079	0.171	0.295	0.451	0.635	0.844	1.080	1.348	1.017	0.786	0.583	0.404	0.256	0.140	0.058	0.010	0.001
T1	2.571	2.587	2.619	2.633	2.624	2.608	2.617	2.630	2.657	2.715	2.652	2.628	2.622	2.619	2.635	2.630	2.605	2.577	2.570
T2	2.677	2.689	2.725	2.796	2.911	3.062	3.241	3.444	3.660	3.868	3.605	3.388	3.191	3.016	2.875	2.772	2.710	2.680	2.675
T3	3.162	3.166	3.168	3.177	3.222	3.305	3.423	3.565	3.740	3.976	3.691	3.526	3.390	3.277	3.205	3.172	3.170	3.164	3.162
0.0000	3.266	3.274	3.309	3.383	3.493	3.632	3.798	3.988	4.206	4.456	4.147	3.935	3.751	3.591	3.459	3.357	3.294	3.269	3.266
0.0000	3.332	3.349	3.400	3.484	3.601	3.750	3.928	4.132	4.363	4.518	4.300	4.074	3.877	3.705	3.565	3.456	3.381	3.340	3.333
0.0000	3.705	3.727	3.785	3.877	4.000	4.155	4.253	4.326	4.409	4.627	4.395	4.313	4.251	4.111	3.963	3.846	3.763	3.715	3.706
0.0000	3.750	3.772	3.829	3.917	4.036	4.165	4.308	4.478	4.677	4.908	4.619	4.427	4.256	4.117	4.001	3.888	3.807	3.760	3.751
0.0000	3.863	3.879	3.903	3.962	4.050	4.185	4.338	4.544	4.763	4.998	4.708	4.489	4.290	4.144	4.017	3.943	3.899	3.873	3.864
0.0000	3.874	3.886	3.944	4.035	4.146	4.185	4.358	4.551	4.777	5.037	4.717	4.500	4.314	4.189	4.122	4.005	3.922	3.879	3.875
0.0000	3.915	3.933	3.984	4.064	4.158	4.309	4.474	4.661	4.869	5.052	4.817	4.610	4.429	4.269	4.140	4.037	3.964	3.922	3.915
0.0000	3.955	3.976	4.033	4.124	4.173	4.314	4.496	4.702	4.870	5.075	4.827	4.647	4.448	4.271	4.148	4.093	4.012	3.964	3.955
0.0000	3.974	4.011	4.084	4.125	4.247	4.402	4.573	4.712	4.904	5.135	4.856	4.673	4.532	4.356	4.208	4.118	4.056	3.991	3.974
0.0000	4.042	4.055	4.108	4.170	4.284	4.423	4.575	4.731	4.936	5.176	4.876	4.690	4.539	4.381	4.249	4.143	4.094	4.052	4.046
1.3682	4.104	4.108	4.114	4.200	4.315	4.454	4.587	4.795	4.985	5.197	4.942	4.737	4.540	4.423	4.285	4.170	4.107	4.106	4.104
0.0000	4.115	4.131	4.182	4.260	4.359	4.455	4.624	4.822	5.030	5.287	4.966	4.767	4.581	4.426	4.331	4.235	4.164	4.122	4.117
T1	3.148	3.155	3.166	3.151	3.112	3.078	3.085	3.106	3.151	3.236	3.141	3.101	3.090	3.092	3.133	3.156	3.156	3.146	3.144

Re-1a:

S0 SCF (a.u.)	-2091.27296	-2091.27242	-2091.2705	-2091.2672	-2091.26267	-2091.25686	-2091.24991	-2091.24198	-2091.23295	-2091.22169	-2091.23069	-2091.23991	-2091.24804	-2091.25522	-2091.26128	-2091.26611	-2091.26967	-2091.27198	-2091.27286
Osc. Str.	90	100	110	120	130	140	150	160	170	180	190	200	210	220	230	240	250	260	270
S0	0.000	0.015	0.067	0.157	0.280	0.438	0.627	0.843	1.089	1.395	1.150	0.899	0.678	0.483	0.318	0.186	0.089	0.027	0.003
T1	2.753	2.767	2.818	2.903	3.009	3.089	3.143	3.192	3.256	3.356	3.282	3.219	3.170	3.114	3.037	2.929	2.835	2.774	2.752
T2	2.778	2.792	2.843	2.930	3.049	3.203	3.389	3.603	3.846	4.145	3.902	3.656	3.438	3.245	3.082	2.956	2.861	2.800	2.778
T3	3.000	3.012	3.050	3.101	3.165	3.267	3.434	3.639	3.875	4.169	3.929	3.688	3.476	3.299	3.184	3.123	3.065	3.021	3.002
0.0092	2.852	2.866	2.919	3.010	3.134	3.293	3.481	3.696	3.940	4.243	3.994	3.747	3.527	3.333	3.167	3.034	2.935	2.872	2.850
0.094	2.967	2.982	3.036	3.126	3.251	3.409	3.597	3.812	4.056	4.359	4.109	3.862	3.642	3.448	3.282	3.150	3.051	2.988	2.965
0.0005	3.577	3.591	3.643	3.733	3.857	4.016	4.203	4.418	4.662	4.880	4.722	4.474	4.255	4.060	3.894	3.762	3.663	3.600	3.578

1e:

S0 SCF (a.u.)	-1107.23576	-1107.23512	-1107.23319	-1107.22991	-1107.2252	-1107.219	-1107.21131	-1107.20221	-1107.19188	-1107.18055	-1107.18922	-1107.19959	-1107.2086	-1107.21621	-1107.2224	-1107.2272	-1107.23059	-1107.23262	-1107.23327
Osc. Str.	0	10	20	30	40	50	60	70	80	90	100	110	120	130	140	150	160	170	180
Rel SCV (eV)	0.000	0.017	0.070	0.159	0.287	0.456	0.665	0.913	1.194	1.503	1.267	0.984	0.739	0.532	0.364	0.233	0.141	0.086	0.068
T1	2.295	2.304	2.325	2.352	2.386	2.421	2.446	2.454	2.432	2.358	2.350	2.389	2.390	2.374	2.351	2.330	2.314	2.306	2.304
T2	2.322	2.334	2.381	2.468	2.596	2.764	2.973	3.221	3.502	3.810	3.575	3.293	3.048	2.841	2.672	2.542	2.450	2.396	2.378
T3	2.995	3.013	3.065	3.154	3.282	3.451	3.660	3.908	4.188	4.473	4.262	3.980	3.734	3.528	3.359	3.229	3.136	3.081	3.063
0.0003	3.545	3.563	3.615	3.704	3.832	4.001	4.210	4.458	4.706	4.912	4.706	4.521	4.285	4.078	3.909	3.779	3.686	3.631	3.613
0.0002	3.545	3.564	3.623	3.725	3.869	4.051	4.260	4.483	4.739	5.047	4.812	4.530	4.318	4.122	3.949	3.811	3.712	3.655	3.638
1.2401	4.284	4.296	4.333	4.392	4.470	4.566	4.676	4.798	4.926	5.070	5.064	4.867	4.712	4.590	4.494	4.421	4.369	4.337	4.327
0.3442	4.396	4.407	4.449	4.526	4.645	4.807	5.011	5.255	5.521	5.723	5.599	5.327	5.085	4.882	4.718	4.595	4.512	4.467	4.454

Re-1e:

S0 SCF (a.u.)	-1539.454	-1539.453	-1539.45076	-1539.448	-1539.443	-1539.437	-1539.428	-1539.419	-1539.40978	-1539.39841	-1539.40712	-1539.41755	-1539.42658	-1539.43422	-1539.43528	-1539.44519	-1539.4486	-1539.45065	-1539.43411
Osc. Str.	0	10	20	30	40	50	60	70	80	90	100	110	120	130	140	150	160	170	180
Rel SCV (eV)	0.000	0.016	0.075	0.156	0.284	0.452	0.689	0.946	1.190	1.499	1.262	0.979	0.733	0.525	0.496	0.226	0.133	0.078	0.528
T1	2.552	2.567	2.623	2.693	2.788	2.878	2.985	3.069	3.105	3.180	3.054	2.988	2.923	2.861	2.930	2.731	2.668	2.623	3.054
T2	2.575	2.591	2.646	2.722	2.844	3.009	3.228	3.481	3.732	4.032	3.801	3.526	3.287	3.084	3.048	2.792	2.701	2.649	3.062
T3	2.735	2.749	2.787	2.834	2.923	3.066	3.285	3.528	3.768	4.065	3.836	3.566	3.331	3.134	3.107	2.871	2.806	2.774	3.176
0.0105	2.637	2.652	2.711	2.791	2.917	3.082	3.304	3.553	3.803	4.100	3.872	3.599	3.361	3.160	3.121	2.865	2.773	2.717	3.167
0.0754	2.773	2.789	2.847	2.927	3.052	3.218	3.454	3.705	3.937	4.234	4.006	3.734	3.496	3.294	3.252	3.000	2.907	2.851	3.272
0.0005	3.364	3.380	3.439	3.518	3.645	3.811	4.010	4.255	4.532	4.829	4.601	4.328	4.090	3.887	3.852	3.593	3.501	3.446	3.946
0.0005	3.506	3.522	3.581	3.662	3.790	3.956	4.171	4.405	4.629	4.897	4.684	4.436	4.214	4.024	3.986	3.733	3.640	3.584	3.961

A:

S0 SCF (a.u.)	-1702.13477	-1702.13395	-1702.13178	-1702.1284	-1702.12382	-1702.11819	-1702.11138	-1702.10369	-1702.09492	-1702.08771	-1702.09733	-1702.10584	-1702.11331	-1702.11992	-1702.12533	-1702.12956	-1702.13261	-1702.13439	-1702.13478		
T1 SCF (a.u.)	-1702.07698	-1702.07619	-1702.07411	-1702.0709	-1702.06658	-1702.06128	-1702.05484	-1702.0476	-1702.03945	-1702.03274	-1702.0417	-1702.04963	-1702.05665	-1702.06293	-1702.06801	-1702.07202	-1702.07492	-1702.07662	-1702.07699		
Osc. Str.	90	100	110	120	130	140	150	160	170	180	190	200	210	220	230	240	250	260	270		
S0	0.000	0.023	0.082	0.174	0.298	0.452	0.637	0.846	1.085	1.281	1.019	0.787	0.584	0.404	0.257	0.142	0.059	0.011	0.000		
T1	1.232	1.253	1.309	1.396	1.511	1.651	1.820	2.004	2.200	2.349	2.147	1.953	1.773	1.608	1.473	1.365	1.287	1.241	1.232		
0.7921	2.600	2.621	2.675	2.740	2.872	3.012	3.183	3.375	3.590	3.765	3.530	3.321	3.135	2.969	2.835	2.730	2.654	2.609	2.600		
T2	2.778	2.785	2.778	2.759	2.697	2.669	2.681	2.715	2.780	2.857	2.757	2.703	2.676	2.670	2.706	2.752	2.783	2.781	2.777		
T3	2.860	2.864	2.901	2.984	3.104	3.254	3.433	3.620	3.787	3.914	3.744	3.571	3.383	3.208	3.065	2.955	2.884	2.860	2.860		
0.0000	3.158	3.180	3.239	3.295	3.353	3.428	3.536	3.681	3.897	4.086	3.834	3.635	3.503	3.402	3.331	3.282	3.217	3.168	3.158		
0.0000	3.262	3.261	3.267	3.331	3.455	3.609	3.794	4.003	4.240	4.386	4.175	3.944	3.742	3.562	3.414	3.299	3.263	3.261	3.261		
0.0000	3.296	3.311	3.365	3.454	3.576	3.727	3.911	4.095	4.254	4.387	4.208	4.055	3.858	3.680	3.536	3.423	3.344	3.302	3.296		
0.0000	3.305	3.327	3.385	3.476	3.599	3.752	3.936	4.119	4.270	4.422	4.230	4.062	3.884	3.705	3.559	3.445	3.363	3.315	3.304		
0.0000	3.584	3.606	3.665	3.733	3.773	3.850	3.963	4.131	4.300	4.436	4.257	4.085	3.930	3.823	3.757	3.724	3.642	3.594	3.584		
0.0000	3.692	3.714	3.721	3.753	3.797	3.891	4.005	4.143	4.355	4.549	4.290	4.095	3.974	3.862	3.783	3.725	3.721	3.702	3.693		
0.0000	3.695	3.720	3.744	3.755	3.878	3.956	4.041	4.156	4.377	4.568	4.312	4.121	4.014	3.939	3.837	3.750	3.750	3.711	3.696		
0.0028	3.702	3.724	3.770	3.859	3.920	4.026	4.208	4.415	4.652	4.807	4.586	4.356	4.156	3.980	3.908	3.829	3.752	3.712	3.702		
0.0000	3.750	3.742	3.782	3.872	3.979	4.131	4.300	4.475	4.663	4.847	4.612	4.426	4.253	4.084	3.940	3.841	3.760	3.741	3.750		
0.0000	3.797	3.767	3.798	3.888	3.994	4.143	4.315	4.519	4.750	4.934	4.684	4.461	4.265	4.098	3.954	3.859	3.775	3.780	3.796		
0.0000	3.799	3.815	3.874	3.900	4.004	4.144	4.326	4.531	4.765	4.941	4.701	4.474	4.274	4.102	3.967	3.894	3.847	3.799	3.799		
T1	1.573	1.594	1.651	1.738	1.856	2.000	2.175	2.372	2.594	2.777	2.533	2.317	2.126	1.955	1.817	1.708	1.629	1.583	1.573		

B:

S0 SCF (a.u.)	-1254.2712	-1254.27028	-1254.26807	-1254.26464	-1254.26	-1254.2542	-1254.24745	-1254.23973	-1254.23099	-1254.22509	-1254.235	-1254.24292	-1254.25029	-1254.25677	-1254.26214	-1254.26634	-1254.26926	-1254.2709	-1254.27112	
T1 SCF (a.u.)	-1254.17427	-1254.17349	-1254.17158	-1254.16865	-1254.16467	-1254.16019	-1254.15457	-1254.15881	-1254.15666	-1254.15471	-1254.158	-1254.15121	-1254.15707	-1254.16217	-1254.16655	-1254.17009	-1254.17259	-1254.174	-1254.17418	
Osc. Str.	90	100	110	120	130	140	150	160	170	180	190	200	210	220	230	240	250	260	270	
S0	0.000	0.025	0.085	0.178	0.305	0.463	0.646	0.856	1.094	1.255	0.998	0.770	0.569	0.393	0.246	0.132	0.053	0.008	0.002	
T1	2.200	2.219	2.264	2.327	2.402	2.464	2.516	2.563	2.611	2.651	2.590	2.544	2.497	2.436	2.368	2.297	2.240	2.206	2.202	
T2	2.874	2.877	2.877	2.864	2.863	2.907	3.014	3.169	3.362	3.497	3.282	3.102	2.965	2.878	2.862	2.870	2.879	2.875	2.875	
T3	3.257	3.244	3.234	3.259	3.328	3.431	3.560	3.709	3.879	3.996	3.810	3.647	3.505	3.384	3.294	3.241	3.236	3.251	3.256	
1.8395	3.323	3.343	3.392	3.466	3.572	3.694	3.835	3.991	4.159	4.267	4.092	3.927	3.776	3.638	3.521	3.430	3.366	3.330	3.324	
0.0000	3.590	3.604	3.640	3.703	3.791	3.907	4.049	4.220	4.422	4.561	4.338	4.149	3.989	3.855	3.751	3.671	3.620	3.594	3.590	
0.0000	3.591	3.616	3.676	3.770	3.895	4.053	4.238	4.406	4.533	4.630	4.478	4.356	4.160	3.983	3.838	3.724	3.644	3.599	3.593	
0.0000	3.890	3.901	3.935	3.989	4.067	4.162	4.277	4.412	4.568	4.676	4.503	4.361	4.228	4.117	4.030	3.962	3.917	3.893	3.891	
0.0000	3.903	3.925	3.982	4.072	4.189	4.233	4.307	4.448	4.686	4.810	4.589	4.363	4.275	4.209	4.138	4.027	3.951	3.910	3.906	
0.0000	3.953	4.012	4.108	4.178	4.192	4.328	4.428	4.553	4.703	4.846	4.641	4.501	4.385	4.277	4.188	4.160	4.062	3.976	3.957	
0.0000	4.113	4.136	4.169	4.201	4.260	4.345	4.525	4.729	4.918	5.042	4.843	4.646	4.450	4.293	4.234	4.172	4.163	4.122	4.114	
0.0631	4.161	4.160	4.189	4.207	4.306	4.426	4.569	4.735	4.964	5.120	4.870	4.666	4.508	4.372	4.258	4.195	4.163	4.158	4.164	
0.3015	4.183	4.187	4.199	4.319	4.472	4.628	4.795	4.976	5.172	5.297	5.093	4.903	4.726	4.564	4.403	4.259	4.188	4.186	4.181	
0.0322	4.282	4.307	4.366	4.457	4.575	4.712	4.850	5.006	5.179	5.300	5.109	4.941	4.792	4.655	4.521	4.412	4.334	4.290	4.285	
0.0000	4.288	4.311	4.369	4.457	4.581	4.718	4.881	5.064	5.274	5.401	5.188	4.988	4.813	4.657	4.524	4.414	4.338	4.295	4.290	
0.0012	4.331	4.354	4.407	4.480	4.592	4.735	4.916	5.120	5.283	5.416	5.215	5.037	4.840	4.666	4.536	4.445	4.380	4.339	4.333	
T1	2.637	2.659	2.711	2.790	2.899	3.021	3.174	3.058	3.117	3.170	3.090	3.265	3.106	2.967	2.848	2.751	2.683	2.645	2.640	

1 W. Perrin, D.; Armarego, *Purification of Laboratory Chemicals*, Pergamosn Press: Oxford, 1998.

2 J. L. Alonso-Gómez, P. Schanen, P. Rivera-Fuentes, P. Seiler and F. Diederich, *Chem. - A Eur. J.*, 2008, **14**, 10564–10568.

3 S. Kulyk, W. G. D. Jr, W. S. Kassel, M. J. Zdilla and S. M. Sieburth, 2011, 4679–4682.

4 Compound (*E*)-**1c** was provided by Hoffmann-La Roche Company.

5 a) P. Hohenberg, W. Kohn, Phys. Rev. 1964, 136, B864. b) W. Kohn, L. Sham, Phys. Rev. 1965, 140, A1133

6 C. Adamo, V. Barone, J. Chem. Phys. 1999, 110, 6158

7 a) Wang, J, Durbeej, B. J Comput Chem. 2020, 41, 1718 b) D. Bousquet, R. Fukuda, D. Jacquemin, I. Ciofini, C. Adamo, M. Ehara, J. Chem. Theory Comput. 2014, 10, 3969 c) D. Jacquemin, V. Wathelet, E.A. Perpète, Carlo Adamo, J. Chem. Theory Comput. 2009, 5, 2420

8 É. Brémond, M. Savarese, N. Qiang Su, Á.J. Pérez-Jiménez, X. Xu, J.C. Sancho-García, C. Adamo, J. Chem. Theory Comput. 2016. 12, 459

9 a) A.L. Fetter, J.D. Walecka, Quantum Theory of Many-Particle Systems, McGraw–Hill, New York, 1971 b) S. Hirata, M. Head-Gordon, Chemical Physics Letters, 1999, 314, 291

10 a) A. Dreuw, M. Head-Gordon, J. Am. Chem. Soc. 2004, 126, 4007 b) A. Chantzis, A.D. Laurent, C. Adamo, D. Jacquemin, J. Chem. Theory Comput. 2013, 9, 4517

11 a) R. Ditchfield, W.J. Hehre, J.A. Pople, J. Chem. Phys. 1971, 54, 724 b) W. R. Wadt, P. J. Hay, J. Chem. Phys. 1985, 82, 270

12 a) F. London, J. Phys. Radium, 1937, 8 , 397 b) R. McWeeny, Phys. Rev., 1962, 126, 1028 c) R. Ditchfield, Mol. Phys., 1974, 27, 789 d) K. Wolinski, J. F. Hilton, P. Pulay, J. Am. Chem. Soc., 1990, 112, 8251 e) J. R. Cheeseman, G. W. Trucks, T. A. Keith, M. J. Frisch, J. Chem. Phys., 1996, 104, 5497